ASSESSMENT AND APPLICATIONS OF ZACHARIASEN'S THEORY OF EXTINCTION

A thesis

presented by

Mehmet Fehmi Oztug

to the

University of St.Andrews

in application for the degree

of Master of Science

DECLARATION

I hereby declare that this thesis has been composed by me, is a record of work done by me and has not been presented for a Higher Degree.

The work was carried out in the research laboratories of the Physics Department, St.Salvator's College, University of St.Andrews, under the supervision of Dr. J.L.Lawrence.

Mehmet Fehmi Oztug

CERTIFICATE

I certify that Mehmet Fehmi Oztug has spent seven terms at research work in the Physical Laboratory of St. Salvator's College, University of St. Andrews, under my direction, that he has fulfilled the conditions of Ordinance No. (St. Andrews) and that he is qualified to submit the accompanying thesis in application for the Degree of Master of Science.

Research Supervisor.

ACKNOWLEDGEMENTS

The auther's thanks are due to Dr. J.L.Lawrence for guidance,advise and discussion.He also wishes to thank Proffessor J.F.Allen for the use of research facilities and Drs.Grant,Killean and Lisher for their help.

Abstract

A review of the work on extinction, mainly Zachariasen's theory, criticism and some applications of this theory, is given.

Extinction effects in large single crystals of D(+) tartaric acid are studied from measurements of integrated intensities using copper and molybdenum radiations. Extinction parameters are deduced from these measurements and the variation of extinction with path length is examined.

An estimate of the average mosaic block size of the crystals used is obtained from measurements of the dislocation density of the material by the x-ray topographic method using a Lang camera and the average mosaic spread of the crystals is obtained from the measurements of diffraction profiles using a two-crystal spectrometer. Zachariasen's parameters are compared with these physically observed values.

It is shown that the measured integrated intensities could be affected by type I secondary extinction in which extinction is governed by the mosaic spread. The possibility of the presence of primary extinction is suggested.

Introduction

The essential aim of crystal structure analysis by x-ray diffraction is to obtain a detailed picture of the contents of the crystal at the atomic level in the form of a three-dimensional electron density map. This map is usually obtained by the following steps:-

1. Measurement of the integrated intensities from the crystal from which the structure factors, which are dependent on the nature of the atoms present and their relative positions within the unit cell, may be deduced.
2. Deduction of the atomic arrangement and calculation of the structure factors corresponding to this arrangement.
3. Refinement of this arrangement until the agreement between the calculated and observed structure factors is within the limits of experimental error.

Therefore, the measurement of accurate structure factors is obviously of very great importance in obtaining electron density maps. The electron density at a point $\bar{r}$ in unit cell is given by

$$\rho(\bar{r}) = \sum_{h} F(\bar{h}) \exp(-2\pi i \bar{h}.\bar{r})$$

where $F(\bar{h})$ is the structure factor and $\bar{h}$ is the diffraction vector.

In the refinement process mentioned above, the position of atoms can be obtained from a least-squares process which involves minimising a function of the difference between observed structure factors and those obtained from the model of the crystal, and any inaccuracies in the observed structure factors would affect the resulting atomic parameters.

In most of the experiments, the structure factors are obtained by measuring the integrated intensities diffracted from a small crystal placed in a monochromatic x-ray beam. The structure factors are obtained from these measurements using the equation:

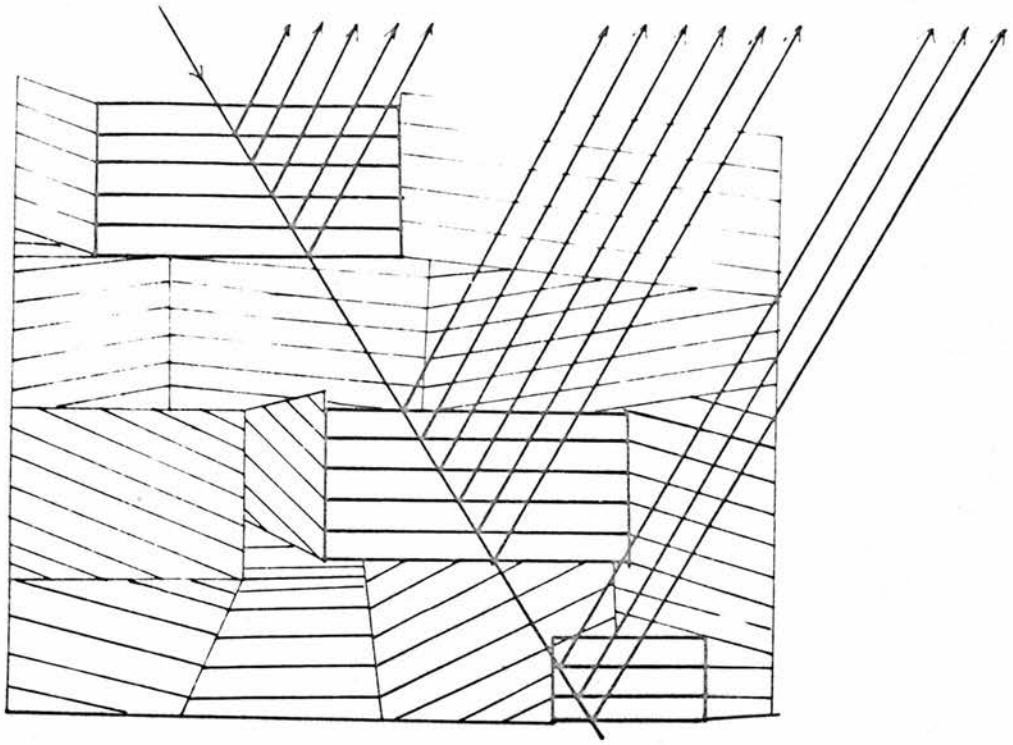

Fig. 2 Mosaic blocks and secondary extinction

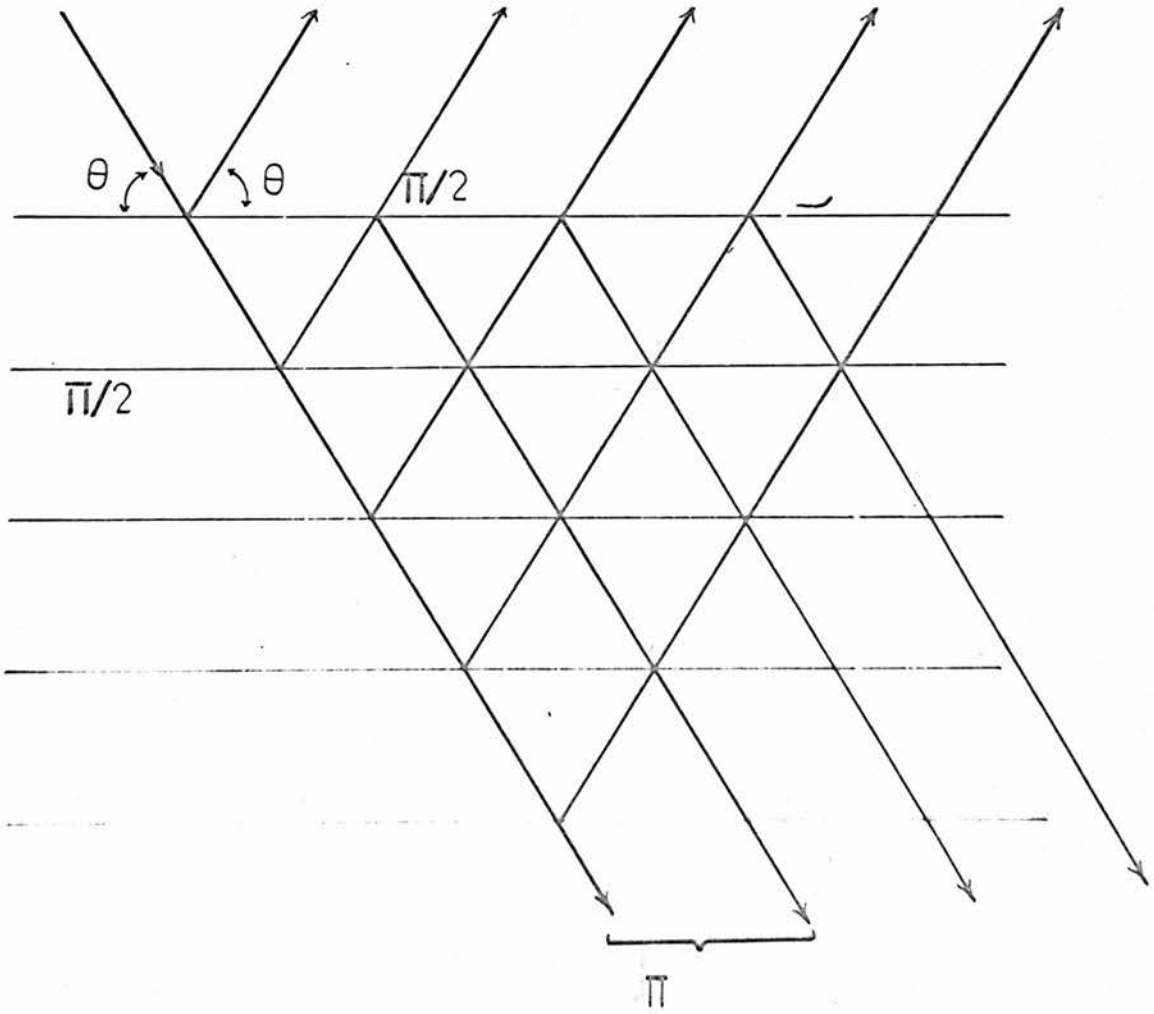

Fig. 1 Primary extinction

$$R = C|F|^2 Lp.A$$

where

R = Integrated intensity

C = Scale factor

F = Structure factor

Lp = Lorentz polarization factor

A = Absorption correction.

The derivation of this equation is from the kinematic theory which is based on the assumption that the intensity of the incident beam is constant at all points within the crystal. No account is taken of the exchange of energy between the incident and diffracted beams and rescattering processes are ignored.

These assumptions are incorrect since the existence of a diffracted beam means that energy has been removed from the incident beam and one should take the rescattering processes and exchange of energy between the incident and diffracted beams inside the crystal, into account. It follows that the values of the structure factors extracted must be incorrect.

In many cases, for many reflections, however, the energy in the diffracted beam is very much less than the main beam and kinematical approximation works quite well. However, when a significant amount of energy is diffracted, the measured structure factors are inevitably smaller than they should be. This effect is referred to as extinction.

This term was first used by Darwin (1914). Using the mosaic block model of a crystal which he proposed and is still used today, it is possible to see how this extinction comes about.

In Darwin's mosaic block model of the crystal, it is assumed that the crystals are composed of large numbers of small domains which are called mosaic blocks. These blocks are assumed to be slightly misoriented from an average orientation, each block being a perfect

crystal region in which coherent scattering takes place, there being no coherence between the beams diffracted from various blocks.

The diffracting planes within each block are well aligned and each part of the block will scatter a fraction of the energy incident upon it into the diffracted beam. Therefore the planes lying deep inside the block receive less energy by the amount diffracted by the preceding atomic planes. Also, the rays which are reflected at the Bragg angle by the planes are directed at the correct angle to be reflected back again into the incident beam by the other planes. Thus, each plane of the crystal rescatters a small fraction of the reflected rays into the incident beam. In every scattering process the phase difference between diffracted and incident beams is $\pi/2$ and, therefore, the twice reflected beams have a phase difference of π from the primary beam, so they weaken the primary beam by destructive interference and the same thing applies to any two beams which have been reflected n and n-2 times respectively. When this phenomenon continues through a large series of planes, the primary beam becomes attenuated. This effect which is taking place inside a single mosaic block was called "primary extinction" by Darwin, fig. (1).

On the other hand, if the diffracting planes of more than one mosaic block are parallel, these blocks will diffract simultaneously and each one of them will scatter a fraction of the incident energy into the diffracted beam. Owing to the energy loss in the incident beam by diffraction at the blocks near the surface, the blocks further inside the crystal having the same orientation are partially shielded by the surface blocks and the energy scattered by these blocks will be less than expected. This phenomenon was called "secondary extinction" by Darwin, fig. (2).

Darwin's model of mosaic structure is an idealized description of the crystal perfection. This model was suggested for the ease of mathematical handling of the problem. A more realistic model for the

problem would give the exact description of the type and geometrical arrangement of imperfections in the crystal but this detailed information is generally not available. Thus the common way is to accept that a real crystal is adequately described by Darwin's model.

As has been mentioned previously, structure factors can be easily determined from the measurements of integrated intensities provided that the diffraction process is kinematic. If a significant amount of energy is being removed by the diffraction process, the kinematic theory no longer applies. Under these circumstances, it is impossible to determine the structure factors from the integrated intensities except in a few examples, e.g. perfect crystal of regular shape. Any least-squares refinement process applied to this data will be invalid since the observed structure factors will be subject to systematic errors although a good agreement may be achieved between the observed and calculated structure factors at the end of the refinement process.

In 1967, an attempt was made by Zachariasen to derive equations based on the mosaic model of Darwin, relating the structure factors to the integrated intensities for real crystals of arbitrary shape when extinction is present. Zachariasen's formulation was widely used and adopted. The first part of this thesis is devoted to a review of the work on extinction, mainly a description and critical analysis of Zachariasen's theory and some of its applications.

In his theory Zachariasen defines two parameters which describe the mosaic block model of a crystal. These are "r" and "g" parameters which are the measures of the mosaic block size and the distribution of the misorientations of mosaic blocks with respect to an average orientation. In the course of extinction corrections, the values of these parameters are deduced and corrections are applied using them.

A necessary condition for the application of Zachariasen's equations must be that these deduced physical parameters should have physically reasonable values. Although mosaic block size can not be very realistic it must at least be an approximate measure of the size of the perfect regions in a real crystal.

In the second part of this thesis, extinction corrections were obtained experimentally on large crystals of tartaric acid, and, following Zachariasen's procedure, the parameters r and g were deduced. Experimental tests were then undertaken to measure these parameters and then to determine whether or not the quantities obtained using Zachariasen's equations have a physical meaning.

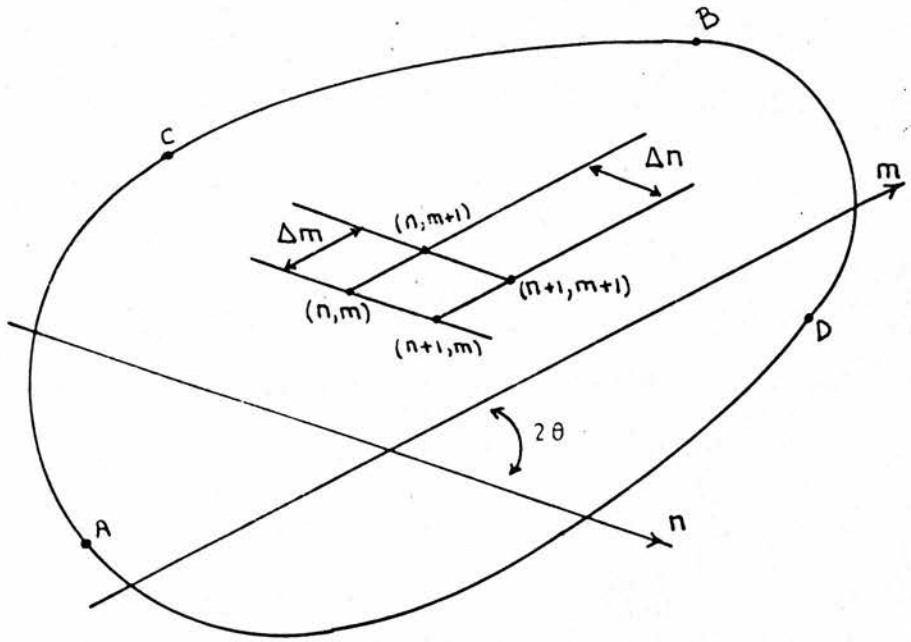
B
C
Δn
m
Δm
(n,m+1)
(n+1,m+1)
(n,m)
(n+1,m)
D
2θ
A
n

Fig. 3

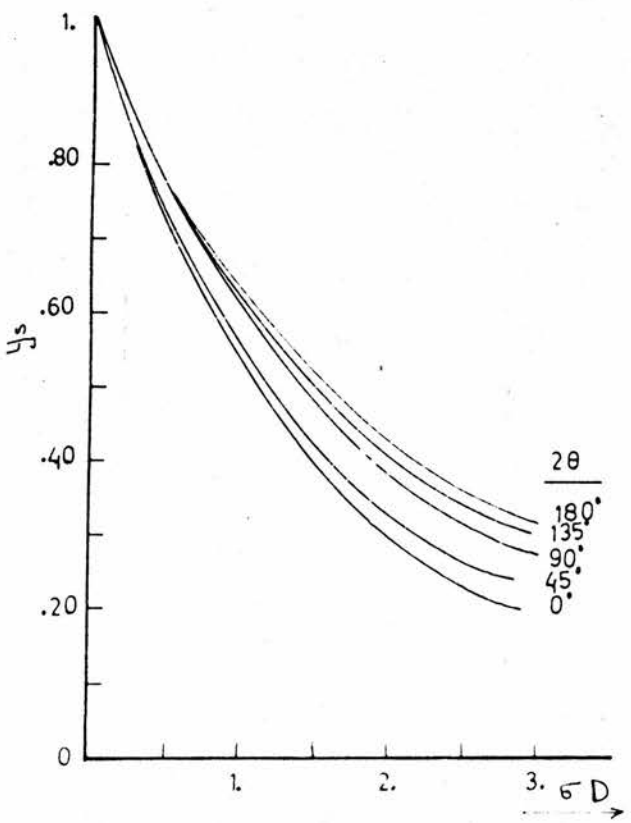
1.
.80
.60
.40
.20
0
1.
2.
3.
σ D
2θ
180°
135°
90°
45°
0°

Fig. 4

CHAPTER I

Zachariasen's paper (1967) entitled "A general theory of x-ray diffraction in crystals" was mainly responsible for the renewal of interest in extinction and the dynamical theory. Previously most of the investigation into extinction had been confined to infinite parallel plates, e.g. Zachariasen (1945), Bacon and Lowde (1948), James (1950).

However, Hamilton (1957) had devised a numerical method of estimating secondary extinction in small, finite crystals which have a uniform cross-section in planes parallel to the plane defined by the incident and diffracted beams. He generalized a pair of differential equations, first given by Darwin (1922) to describe secondary extinction in infinite parallel plates, which described the flow of energy through a crystal.

The power relations between the incident and diffracted beams were expressed as

$$\begin{aligned} (\partial P_H/\partial m) &= \tau P_H + \sigma P_o \\ (\partial P_o/\partial n) &= \tau P_o + \sigma P_H \end{aligned} \qquad (1)$$

where P_o and P_H are the powers of the incident and diffracted beams respectively and $\tau = -(\mu+\sigma)$, where μ is the absorption coefficient and σ is the diffracting power per unit volume and intensity. $\hat{n}$ and $\hat{m}$ are the directions of the incident and diffracted beams respectively.

Hamilton solved the coupled differential equations, eqs. (1), numerically for a convex crystal shown in fig. (3). To obtain this numerical solution, eqs. (1) were replaced by the following difference equations:

$$\begin{aligned} P_H(n,m) &= P_H(n,m-1)[1 + \tau\Delta m] + P_o(n,m-1)\sigma\Delta m \\ P_o(n,m) &= P_o(n-1,m)[1 + \tau\Delta n] + P_H(n-1,m)\sigma\Delta n \ . \end{aligned}$$

Starting from the boundary and using the boundary conditions

$$P_o = P_o^o \qquad \text{along ACB}$$
$$P_H = 0 \qquad \text{along DAC ,}$$

where P_o^o is the power of the incident beam outside the crystal, the values of P_H and P_o can be calculated at all of the points of a grid having a mesh size of $\Delta n \times \Delta m$. The integrated intensity is given by

$$R = h \int_{-\infty}^{\infty} R(\Delta\theta)\, d(\Delta\theta) / \int_{-\infty}^{\infty} W(\Delta\theta)\, d(\Delta\theta)$$

where h is the height of the crystal. If $P_H(a) \ldots P_H(k)$ are the values of P_H calculated by the above numerical method, corresponding to the grid points lying on the exit surface, then $R(\Delta\theta)$ is given by

$$R(\Delta\theta) = \left[\frac{P_H(a) + P_H(k)}{2} + \sum_{i=b}^{k-1} P_H(i)\right] \Delta n \sin 2\theta \ .$$

$W(\Delta\theta)$ is the distribution function for mosaic block alignment. Assuming a distribution function, such that

$$W(\Delta\theta) = \begin{cases} 1/2\eta\sqrt{3} & |\Delta\theta| \leq \eta\sqrt{3} \\ 0 & |\Delta\theta| > \eta\sqrt{3} \end{cases} \qquad (2)$$

where η is the mosaic spread parameter, Hamilton obtained the integrated intensity as:

$$R = h 2\eta\sqrt{3} [R(\Delta\theta)]_{\Delta\theta=0} \ .$$

The secondary extinction correction y_s was obtained as

$$y_s = R/Q'VA$$

where $Q' = Q.y_p = \left(\frac{e^2}{mc^2}\right)^2 \frac{F^2 K^2}{V^2} \frac{\lambda^3}{\sin 2\theta}$. y_p is the primary extinction correction and the other symbols have their usual meanings. The desired accuracy in P_H can be obtained by choosing a sufficiently small mesh size. The couple of differential equations (eqs. 1) can be solved exactly for the limiting cases of $2\theta = 0$ and $2\theta = 180^o$.

Hamilton calculated the secondary extinction corrections y_s, for cylindrical crystals, having diameter D, for 2θ = 0, 45, 90, 135 and 180° cases. The grid size was so chosen that the error in the calculation of y_s was less than 3%. The results of these calculations were presented by means of curves shown in fig. (4) which are a plot of y_s versus σD. From these curves, Hamilton noted that there was an angle dependence, which was negligible for only small extinction ($y_s > 0.7$), and this angle dependence became very important for severe extinction.

Hamilton carried out the same calculations for crystals having a rectangular cross-section in planes parallel to the plane defined by the incident and diffracted beams and concluded that the extinction effects became much more complicated because in this case extinction is a function of the crystal setting as well as of the Bragg angle.

Further, Hamilton noted that the intensities for intense reflections reach a limit as σD increases. The intensity is then no longer dependent on the value of $|F|^2$ but on the size of the crystal and the Bragg angle. It was suggested that this saturation phenomena be used in the determination of η if this limiting value is observed. The limiting values of the integrated intensities were given as

$$\text{For } 2\theta = 180^\circ \qquad R_{lim} = 2\sqrt{3}\, hD\eta$$

$$\text{For } 2\theta = 0^\circ \qquad R_{lim} = \sqrt{3}\, hD\eta \ .$$

Therefore, the method for extinction correction in cylindrical crystals, suggested by Hamilton consists of:

1. Determination of η in the region $y_s > 0.7$ using the approximation $y_s \simeq \exp(-8\sigma D/3\pi)$ or using the limiting values mentioned above if they are observed.

2. Using this value of η, determination of y_s curve for any reflection in the intermediate range, using numerical integration over a grid as described above.

Hamilton applied this method of extinction correction to the observed values of y_s in a neutron diffraction experiment for a single crystal of Fe_3O_4 and obtained very good agreement between the calculated and observed values of y_s.

Later, Hamilton (1963) improved the calculation of P_H values introducing a modified Euler integration scheme instead of previous rectangular grid and the tables of secondary extinction corrections for equatorial reflections from cylindrical crystals were presented.

Zachariasen (1967) developed a general theory of x-ray diffraction for real finite crystals of arbitrary shape and this theory is based on Darwin's mosaic block model of a crystal. He considered first diffraction from a small, perfect crystal, and then from a real crystal, assuming the real crystal to be a distribution of small, independent perfect crystal regions which were slightly misaligned to each other. It was assumed that the normals to the diffracting planes of the individual perfect crystals obeyed an isotropic Gaussian distribution given by

$$W(\Delta) = \sqrt{2}\, g \exp(-2\pi g^2 \Delta^2) \qquad (3)$$

where Δ is the angular deviation from the mean orientation and g is the mosaic spread parameter.

The extinction factor y is defined as being the ratio between the integrated intensity from the real crystal, R, to that obtained by the kinematic theory, R_k.

$$\text{i.e.} \qquad y = R/R_k \qquad (4)$$

and R_k is given by

$$R_k = J_o\, \nu\, A(\mu) Q \qquad (5)$$

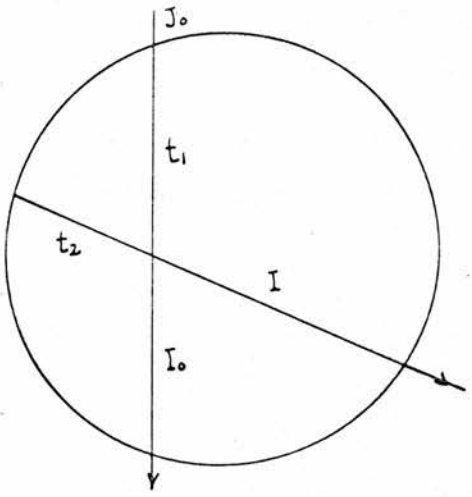

Fig. 5

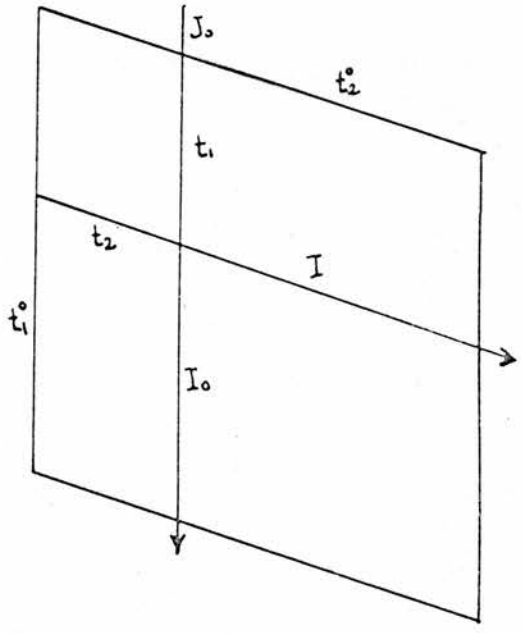

Fig. 6

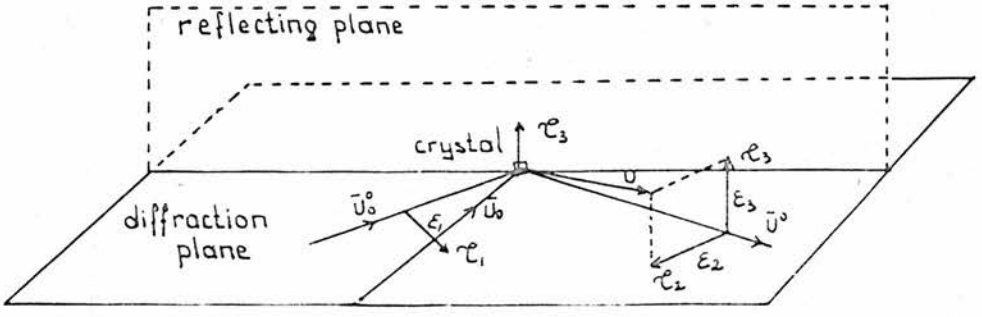

Fig.7

where J_o = Incident beam intensity

ν = Volume of the crystal

$A(\mu)$ = Absorption factor

$Q = \left(\frac{r_o F K^2}{V}\right) \frac{\lambda^3}{\sin 2\theta}$ for x-ray diffraction

$r_o = \left(\frac{e^2}{mc^2}\right)$ = radius of the electron

F = Kinematic structure factor

K = Polarization factor

V = Volume of the unit cell

λ = Wavelength of the radiation

θ = Bragg angle.

Zachariasen used a pair of differential equations similar to those used by Hamilton, and solved these equations for crystals of various shapes. Assuming negligible absorption, he used the equations in the form -

$$\frac{\partial I_o}{\partial t_1} = -\sigma I_o + \sigma I \qquad (6a)$$

$$\frac{\partial I}{\partial t_2} = -\sigma I + \sigma I_o \qquad (6b)$$

I_o and I are the values of the incident and the diffracted intensities inside the crystal, t_1 and t_2 are lengths in the incident and diffracted beams and σ is the diffracting power of the diffracting planes, (fig. 5).

Eq. (6a) represents the variation in intensity of the main beam as it passes through the crystal. Energy is removed from the beam by the diffraction process, $(-\sigma I_o)$, and the second term (σI) represents the rescattering of the diffracted beam back into the main beam. Eq. (6b) represents the variation in intensity of the diffracted beam and the summation of the two equations expresses the energy conservation for the process, i.e.,

$$\frac{\partial I_o}{\partial t_1} + \frac{\partial I}{\partial t_2} = 0 \ .$$

The boundary conditions are:

$$I_o = J_o \quad \text{at} \quad t_1 = 0$$
$$I = 0 \quad \text{at} \quad t_2 = 0 \ .$$

From these equations, the power of the diffracted beam, $P(\varepsilon_1)$, at some angular deviation ε_1 from the ideal Bragg angle, can be obtained from:

$$P(\varepsilon_1) = \oint I \, \bar{u} . d\bar{s} = \int \frac{\partial I}{\partial t_2} \, dv$$

where $\bar{u}$ is the diffracting direction and $d\bar{s}$ is a surface element of the crystal. A function $\phi(\sigma)$ was introduced such that:

$$P(\varepsilon_1) = J_o \, v\sigma\phi(\sigma)$$

and, since the total integrated intensity is given by

$$R = \int P(\varepsilon_1) \, d\varepsilon_1 \ ,$$

the extinction factor y can, in principle, be obtained from

$$y = Q^{-1} \int \sigma\phi(\sigma) \, d\varepsilon_1 \ . \qquad (7)$$

The problem is then to find $\phi(\sigma)$ as the solution of eqs. (6a) and (6b), and to find y using eq. (7).

When all extinction effects are neglected, the solution to eqs. (6a) and (6b) gives the kinematic approximation

$$y = \frac{P}{P_k} = 1 \ .$$

Neglecting the "feedback" term σI in eq. (6a) gives an exponential solution

$$I_o = J_o \exp(-\sigma t_1)$$

$$I = J_o[1 - \exp(-\sigma t_2)]\exp(-\sigma t_1)$$

and $$P = J_o \nu\sigma A(\sigma)$$

where $$A(\sigma) = 1 - \sigma\bar{t} + \tfrac{1}{2}\sigma^2\bar{t}^2 - \frac{1}{6}\sigma^3\bar{t}^3 + \ldots$$

and $$\overline{t^n} = \nu^{-1} \int (t_1 + t_2)^n \, d\nu \, .$$

This particular solution is very similar to the exponential solution suggested by Bragg, James and Bosanquet (1921), where the extinction can be considered as an increase in the absorption term of the form $\exp -(\mu + gQ)t$.

For arbitrary shape, Zachariasen obtained the power series solution of eqs. (6a) and (6b) as an expression for $\frac{\partial I}{\partial t_2}$

$$\frac{\partial I}{\partial t_2} = \sigma J_o \sum_n \frac{(-\sigma)^n}{n!} t^{(n)} \tag{8}$$

where $$t^{(n)} = \sum_j \binom{n}{j} t_1^{n-j} t_2^j \, .$$

Zachariasen used this general result in eq. (8) to find the function $\phi(\sigma)$ for different shapes. For a parallelopiped, having three equal edges, two of them being parallel to the incident and diffracted beams and the third, being perpendicular to the plane of incidence, fig. (6), he obtained $\phi(\sigma)$ as

$$\phi(\sigma) = 1 - \sigma t_o + (5/6)(\sigma t_o)^2 - (7/12)(\sigma t_o)^3 + \ldots \tag{9}$$

where t_o is the length of the edge of the parallelopiped.

The same procedure was carried out for a sphere of radius r, for small scattering angles, giving the results:

Forward direction:

$$\phi(\sigma) = 1 - \sigma\bar{t} + (16/15)(\sigma\bar{t})^2 - (80/81)(\sigma\bar{t})^3 \tag{10}$$

Backward direction:

$$\phi(\sigma) = 1 - \sigma\bar{t} + (64/45)(\sigma\bar{t})^2 \ldots \tag{11}$$

where $\bar{t} = (3/2)r$.

Eq. (10) was derived for small scattering angles. However, since $\sigma\bar{t} << 1$ at large scattering angles, Zachariasen suggested that eq. (10) can be used as a general expression for a sphere.

Eqs. (9), (10) and (11) show that $\phi(\sigma)$ depends on the shape of the crystal. Further, comparison of eqs. (10) and (11) indicates that $\phi(\sigma)$ may have a significant angle dependence. However, from the form of these results Zachariasen, suggested an approximation for any arbitrary shape as

$$\phi(\sigma) = \frac{1}{1+\sigma\bar{t}} . \tag{12}$$

According to Zachariasen, eq. (12) is exact for infinite parallel plate for symmetrical Bragg case and a very good approximation for a sphere, but a poor approximation for a parallel plate in the symmetrical Laue case, because in this case the power is equally divided between transmitted and diffracted beams.

In obtaining the diffracting power, Zachariasen assumed that it may be correctly obtained from kinematic theory i.e.

$$\sigma(\varepsilon_1) = J_o^{-1} \nu^{-1} P_k(\varepsilon_1) . \tag{13}$$

The geometry of diffraction is shown in fig. (7). The direction of incidence, $\bar{u}_o$, is given by

$$\bar{u}_o = \bar{u}_o^o - \varepsilon_1\bar{\tau}_1$$

where $\bar{u}_o^o$ is the ideal Bragg direction and $\bar{\tau}_1$ is a unit vector in the plane of incidence perpendicular to $\bar{u}_o^o$. The direction of diffraction, $\bar{u}$, is given by

$$\bar{u} = \bar{u}^o + \varepsilon_2\bar{\tau}_2 + \varepsilon_3\bar{\tau}_3$$

where $\bar{u}^o$ is the ideal diffraction direction and

$$\bar{u}^o - \bar{u}_o^o = \lambda\bar{H}$$

where $\bar{H}$ is the reciprocal lattice vector associated with the diffracted beam. The diffraction vector $\bar{S}$ is then

$$\bar{S} = \frac{2\pi}{\lambda}(\bar{u} - \bar{u}_o)$$
$$= 2\pi\bar{H} + \overline{\Delta s}$$

where $\Delta s = \frac{2\pi}{\lambda}(\varepsilon_1\bar{\tau}_1 + \varepsilon_2\bar{\tau}_2 + \varepsilon_3\bar{\tau}_3)$.

The intensity in the direction $(\bar{\varepsilon}_1, \bar{\varepsilon}_2, \bar{\varepsilon}_3)$ is given by

$$I_k(\varepsilon_1,\varepsilon_2,\varepsilon_3) = J_o \left|\frac{e^2 F K}{mc^2 R}\right|^2 \left|\Sigma \exp(i\overline{\Delta s}.\bar{L})\right|^2 \qquad (14)$$

where L is a lattice vector and R is the distance from the crystal to the counter. Then, $P_k(\varepsilon_1)$ becomes:

$$P_k(\varepsilon_1) = R^2 \iint I_k \, d\varepsilon_2 \, d\varepsilon_1 \, . \qquad (15)$$

In general, $\sigma(\varepsilon_1)$ depends on the shape of the crystal and one should solve the summations and integrations in eq. (14) and eq. (15) for the particular shape. Then $\sigma(\varepsilon_1)$ can be calculated from eq. (13).

Zachariasen calculated $\sigma(\varepsilon_1)$ for a particular case of the parallelopiped of fig. (6) again assuming all of the edges t_1^o, t_2^o, t_3^o are equal to t_o and obtained the result as a delta function i.e.

$$\sigma(\varepsilon_1) = Q\alpha \frac{\sin^2 \pi\alpha\varepsilon_1}{(\pi\varepsilon_1\alpha)^2} \qquad (16)$$

where $\alpha = \frac{t_\perp}{\lambda}$ and $t_\perp = |\bar{t}_2^o \times \bar{u}_o| = t_o \sin 2\theta$.

As mentioned above, $\sigma(\varepsilon_1)$ is dependent on the shape of the crystal and may be very complicated for an arbitrary shape. However Zachariasen assumed that eq. (16) is reasonable for any symmetrical shape, especially for a spherical crystal. In eq. (16) the only shape dependent factor is $t_\perp$. For infinite parallel plate $t_\perp$ is given as $D_o \sin\theta$ for the Laue case and $D_o \cos\theta$ for the Bragg case, where D_o is the thickness of the crystal. For a sphere of radius r, $t_\perp$ is equal to $(\frac{3}{2})r$.

In the evaluation of the integral in eq. (7), it is convenient to replace the delta function form of eq. (16) by an equivalent expression of Poisson form. Zachariasen assumed that

$$\sigma = \frac{a}{1+b^2\varepsilon_1^2} ,$$

$$\int \sigma \, d\varepsilon_1 = Q ,$$

and

$$\int \sigma^2 \, d\varepsilon_1 = \frac{3}{2} Q^2 \alpha$$

and so obtained the approximate expression for $\sigma(\varepsilon_1)$, for arbitrary symmetrical shapes, as

$$\sigma(\varepsilon_1) \cong \frac{4/3Q\alpha}{1 + (\frac{4\pi}{3} \alpha\varepsilon_1)^2} . \tag{17}$$

Then, substituting eq. (17) and eq. (12) in eq. (7), the expression for y becomes

$$y = (1 + 2x)^{-\frac{1}{2}} = 1 - x + (3/2)x^2 - (5/2)x^3 + \ldots \tag{18}$$

where $x = \frac{2}{3} Q\alpha\bar{t}$ and $\bar{t}$ is the mean path length through the crystal.

For various crystal shapes, Zachariasen listed the x values as

Symmetrical Laue case: $$x = \frac{\left|\frac{e^2 F K \lambda D_o}{mc^2 V}\right|^2}{3 \cos^2\theta} \tag{19a}$$

Symmetrical Bragg case: $$x = \frac{\left|\frac{e^2 F K \lambda D_o}{mc^2 V}\right|^2}{3 \sin^2\theta} \tag{19b}$$

Parallelopiped of fig. (6): $$x = \frac{2\left|\frac{e^2 F K \lambda t_o}{mc^2 V}\right|^2}{3} \tag{19c}$$

Sphere of radius r: $$x = \frac{\left|\frac{e^2 F K \lambda r}{mc^2 V}\right|^2}{2 \sin 2\theta} \tag{19d}$$

For infinite parallel plate case, the exact results of the dynamical theory are available. They are given as:

For symmetrical Laue case: $y = 1 - x + (9/20)x^2 - (3/28)x^3 + \ldots$

For symmetrical Bragg case: $y = 1 - x + (6/5)x^2 - (51/35)x^3 + \ldots$

where x values are given by eqs. (19a) and (19b) respectively.

For symmetrical Laue case Zachariasen's theory does not agree with the findings of the dynamical theory. According to Zachariasen, this is a natural consequence of the approximation, eq. (12), which is a poor approximation for Laue case. But when the Bragg case is considered, if the delta function form, eq. (16) is used,

$$y = 1 - x + (5/4)x^2 - (13/8)x^3 + \ldots$$

which agrees very well with the dynamical results. According to Zachariasen, this satisfactory agreement suggests that the findings of the theory are acceptable approximations.

Eq. (18) can be used to determine the lower limit of crystal size for negligible primary extinction. If the integrated intensity can be measured to an accuracy of two per cent then the applicability of the kinematical approximation (y=1) for primary extinction is restricted to a range $x < 0.02$ and this requires a spherical crystal of radius $r < 0.5 \times 10^{-4}$ cm for most of the specimen crystals, for strong reflections.

The theory relating extinction in a single perfect crystal was then extended by Zachariasen to deal with real crystals of the Darwin mosaic block model. The domains are assumed to be all of the same size and nearly spherical in shape. The mean path length of the x-rays through each domain is $\bar{t} = 3/2\ r$ where r is the mean domain radius. The crystal is assumed to contain a large number of these domains and their orientations are governed by eq. (3).

The half width of the distribution function is given by

$$W_{\frac{1}{2}} = g^{-1}[\log(2/2\pi)]^{\frac{1}{2}} = 0.332\ g^{-1}. \qquad (20)$$

From the eq. (16) or eq. (17) the half width of the diffraction pattern is given as

$$(\varepsilon_1)_{\frac{1}{2}} = 0.295\ \lambda\ r^{-1} = 0.443/\alpha$$

or (21)

$$(\varepsilon_1)_{\frac{1}{2}} = (1/2\pi)\ \lambda\ r^{-1} = (3/4\pi)\ \alpha^{-1} \ .$$

The diffraction in real crystal is treated in the same manner as in the perfect crystal. The basic equations eq. (6a) and eq. (6b) are the same, except the use of convoluted value $\bar{\sigma}$ instead of σ and the use of $\bar{T}$ which is the mean path length through the crystal, instead of $\bar{t}$, which is the mean path length through a mosaic block. $\bar{\sigma}(\varepsilon_1)$ is defined as

$$\bar{\sigma}(\varepsilon_1) = \int W(\Delta)\ \sigma(\varepsilon_1 + \Delta)d\Delta \ .$$

Assuming

$$\sigma(\varepsilon_1) \cong Q\ \alpha\ \exp(-\pi\alpha^2 \varepsilon_1^{\,2})$$

and

$$\bar{\sigma}(\varepsilon_1) \cong Q\ \alpha' \frac{\sin^2 \pi\alpha'\varepsilon_1}{(\pi\alpha'\varepsilon_1)^2} \qquad (22)$$

where $\alpha' = \sqrt{2}\ \alpha/\sqrt{\alpha^2 + 2g^2}$,

and, using the approximation

$$3g/2 \cong \sqrt{2}\ g \ ,$$

it follows that

$$\bar{\sigma}(\varepsilon_1) \cong \frac{(4/3)\ Q\ \alpha'}{1 + [\frac{4\pi}{3}\ \alpha'\varepsilon_1]^2} \qquad (23)$$

where $\alpha' \cong \alpha/\sqrt{1 + (2\alpha/3g)^2}$.

Eq. (22) and eq. (23) are precisely analogous to eq. (16) and eq. (17) respectively which were derived for the parallelopiped of fig. (6) for the perfect crystal case. In eq. (23) when $\alpha >> g$, α'

is given by (3/2)g and, when $\alpha << g$, $\alpha' \cong \alpha$.

Solution of the basic equations in the case of real crystal is very similar to the perfect crystal case, giving the result

$$\phi(\bar{\sigma}) = \frac{1}{1+\bar{\sigma}\bar{T}} \tag{24}$$

which is precisely analogous to eq. (12) and leads to

$$y = (1+2x)^{-\frac{1}{2}}$$

where $$x = \frac{2}{3} Q \alpha' \bar{T}$$

if $\bar{t}$ is small compared with $\bar{T}$.

In order to include the effect of absorption, Zachariasen rewrote the basic equations as:

$$\frac{\partial I_o'}{\partial T_1} = - (\mu+\sigma) I_o' + \sigma I'$$

$$\frac{\partial I'}{\partial T_2} = - (\mu+\sigma) I' + \sigma I_o' \ .$$

Solution for severe absorption is complicated. According to Zachariasen, the solution to these equations, in the case of small absorption, can be expressed in terms of the solution of eq. (6)

$$I' \cong I \exp[- \mu(T_1 + T_2)] = I \, e^{-\mu \bar{T}} = I \, A(\mu)$$

where $A(\mu)$ is the transmission factor. Then

$$\bar{T} = - A^{-1} \frac{dA}{d\mu} \ . \tag{25}$$

Therefore, according to Zachariasen, if the effective mean path length, which is generally given by

$$\bar{T} = \frac{1}{A(\mu)} \int_\tau (T_1 + T_2) \exp(- \mu(T_1 + T_2)) \, d\tau \ ,$$

is calculated from eq. (25), the effects of absorption on extinction will be accounted for automatically.

Effects of polarization are included in the theory as well. If the incident radiation is unpolarized, k=1 for vertical component and k = cos2θ for parallel component of polarization.

Therefore, for parallel component

$$x_{//} = x_o \cos^2 2\theta \quad \text{and} \quad Q_{//} = Q_o \cos^2 2\theta$$

where x_o and Q_o are the values of x and Q respectively, without any polarization effect. For the integrated intensity

$$R_{//} = J_o \nu Q_o \cos^2 2\theta \, y_{//}$$

and

$$R_{\perp} = J_o \nu Q_o y_{\perp} .$$

On the other hand

$$R = R_k y$$

where

$$R_k = J_o \nu Q_o p_1$$

and p_1 is given by

$$p_1 = \frac{1 + \cos^2 2\theta}{2} .$$

$$\therefore \quad R = J_o \nu Q_o p_1 y = J_o \nu Q_o \frac{(1 + \cos^2 2\theta)}{2} y .$$

The average value of R is then

$$R = \frac{R_{\parallel} + R_{\perp}}{2} = J_o \nu Q_o \frac{(y_{\perp} + y_{//} \cos^2 2\theta)}{2} .$$

From this

$$(\frac{1 + \cos^2 2\theta}{2})y = y_{\perp} + y_{//} \cos^2 2\theta \qquad \text{and}$$

$$y = \frac{y_{\perp} + y_{//} \cos^2 2\theta}{1 + \cos^2 2\theta}$$

where

$$y_{\perp} = (1 + 2x_o)^{-\frac{1}{2}}$$

and

$$y_{//} = (1 + 2k^2 x_o)^{-\frac{1}{2}} .$$

Therefore,

$$y = \frac{(1 + 2x_o)^{-\frac{1}{2}} + (1 + 2k^2 x_o)^{-\frac{1}{2}} k^2}{1 + k^2} .$$

According to Zachariasen, for $x_o >> 1$, the above equation can be approximated as

$$y \cong \frac{1 + k}{\sqrt{2x_o}\,(1+k^2)}$$

and for $x_o < 5$, without introducing important error,

$$y \cong (1 + 2 \frac{p_2}{p_1} x_o)^{-\frac{1}{2}} \qquad (26)$$

where $$\frac{p_2}{p_1} = (1 + k^4)/(1 + k^2) .$$

When $\bar{t}$ is not negligible compared to $\bar{T}$, x_o should be replaced by its mean value $\bar{x}_o$ which is given by

$$\bar{x}_o = (2/3)\, Q_o \alpha [\bar{t} + (\bar{T}-\bar{t})/\sqrt{1 + (2\alpha/3g)^2}\,]$$

where $\frac{2}{3} Q_o \alpha \bar{t}$ and $\frac{2}{3} Q_o \alpha (\bar{T}-\bar{t})/\sqrt{1 + (2\alpha/3g)^2}$ corresponds to primary and secondary extinction respectively.

For the general case, the findings of Zachariasen's theory can be summarised as

$$R = R_k\, y = J_o\, Q_o\, p_1\, \nu\, A(\mu)\, y$$

$$y = (1 + 2 \frac{p_2}{p_1} \bar{x}_o)^{-\frac{1}{2}} \qquad (27)$$

where $$\bar{x}_o = \beta\, Q_o [\bar{t} + (\bar{T}-\bar{t})/\sqrt{1 + (\beta/g)^2}\,] ,$$

$$\beta = 2\bar{t}_\perp / 3\lambda ,$$

and $$\bar{t}_\perp = (3/2)r \quad \text{for a spherical crystal.}$$

As mentioned before, primary extinction can be neglected for $x_o < 0.02$ corresponding to a mosaic block radius of $r < 0.5 \times 10^{-4}$ cm. When primary extinction is neglected, $\bar{x}_o$ reduces to

$$x_o = r\lambda^{-1} Q_o \bar{T}/\sqrt{1+(r/\lambda g)^2} \qquad (28)$$

representing only secondary extinction and according to Zachariasen, this is the case in most experiments.

Zachariasen introduced two important limiting types of crystals. In one of them, $r/\lambda g >> 1$, which means that the distribution function is much wider than the diffraction pattern from a single mosaic block. In this case, secondary extinction is dependent on the parameter g. This type is called a type I crystal. For this type, x_o is given as

$$x_o = g Q_o \bar{T} .$$

The other type, in which $(r/\lambda g) << 1$, is called a type II crystal. In this type, the diffraction pattern from a single mosaic block is greater than the width of the distribution function W. In this case the size of the mosaic blocks govern the amount of secondary extinction and x_o is given by

$$x_o = r\lambda^{-1} Q_o \bar{T} .$$

If data from two wavelengths are available, the extinction parameters obtained from each wavelength data set can be compared and the crystal categorized into either type I or type II or an intermediate type. In the case of the intermediate type, $r\lambda^{-1}$ and g are of the same magnitude and x_o is given by eq. (28).

Zachariasen noted that in the previous work on extinction and on the determination of the parameter g, many authors assumed that the crystals are of type I. Zachariasen suggested that in some, and maybe in most of the cases, the crystals are of type II.

In this theory, Zachariasen made some approximations. For example, it is assumed that the basic equations are correct in describing the flow of energy inside the crystal, that equations (12), (24), (17) and (23) are approximate forms, that the Laue form of the peak profile function can be replaced by the Poisson function, and

that the effects of absorption are taken into account by using an effective path length $\bar{T}$ defined by eq. (25).

Because of the approximations involved, Zachariasen suggested the functions

$$y = \tanh \sqrt{3x}/\sqrt{3x}$$
$$y = \tan^{-1} \sqrt{3x}/\sqrt{3x} \qquad (29)$$

as alternatives to eq. (18) for the form of y. All these suggested functions cannot be distinguished theoretically, they cannot be distinguished when x is small, but for $x >> 1$ there are significant differences between them.

Therefore this attempt of Zachariasen to cover the entire range of crystalline perfection by his general formulas for extinction in real crystals needs to be tested experimentally. Zachariasen (1968) tested the validity of the general formulas experimentally for two crystals namely for hambergite and α-quartz crystals.

In Zachariasen's procedure, eq. (27) is rewritten as $x_o = \lambda^{-1} Q_o \bar{T} r^*$ where $r^* = r/\sqrt{1+(r/\lambda g)^2}$ and therefore

$$x = (P_2/P_1)\, Q_o\, \lambda^{-1}\, \bar{T}\, r^* \ . \qquad (30)$$

The extinction correction may be applied either to the calculated structure factors $|F_c|$ or to the observed structure factors $|F_o|$. Then one has;

$$|F_o| = C\, |F_c|\, [1 + 2x]^{-\frac{1}{4}} \qquad (31)$$

or

$$|F_c| = C^{-1}\, |F_o|\, \sqrt{x^*} + \sqrt{1 + x^{*2}} \qquad (32)$$

where

$$x^* = x/\sqrt{1+2x} \ .$$

Then, Zachariasen's suggestion for extinction correction is to find the scale factor C from weak reflections (zero or small extinction) and then using eq. (30) to obtain r^* for strong and extinguished reflections. If the structure parameters of the crystal are not known with sufficient accuracy, it is necessary to carry out a least squares refinement based on eq. (31) or eq. (32) with r^* as an additional parameter in the refinement.

If the measurements of the integrated intensities are carried out by using two different wavelengths, it is possible to find out both parameters r and g, which are characteristics of the crystal specimen. If r_1^* and r_2^* are two values corresponding to different wavelengths λ_1 and λ_2, then r and g are given as

$$r = r_1^* r_2^* \sqrt{(\lambda_1^2 - \lambda_2^2)/(\lambda_1^2 r_2^{*2} - \lambda_2^2 r_1^{*2})}$$

$$g = (r_1^* r_2^*/\lambda_1\lambda_2) \sqrt{(\lambda_1^2 - \lambda_2^2)/(r_1^{*2} - r_2^{*2})} \quad . \tag{33}$$

In this way, the type of the crystal can be determined. In type I, since $r\lambda^{-1} \gg g$, $r^* \approx \lambda g$ and in type II; $r\lambda^{-1} \ll g$, so $r^* \approx r$.

Zachariasen calculated r^* values for samples of hambergite and of α-quartz crystals, using both M_oK_α and C_uK_α radiations and worked out the parameters r and g, finding in both cases that the crystals were of type II.

Further, he found out that the formula $y = (1+2x)^{-\frac{1}{2}}$ gives more consistent results (i.e. r^* is not dependent on the amount of extinction) compared to the other two suggested functions given in eq. (29).

In the analysis of the fluctuations of individual r^* values from the mean in both crystals, Zachariasen noted that fluctuations have the same sign, suggesting the discrepancies in eq. (31) are not due to experimental errors, but due to departures from the spherical symmetry of electron distribution due to band formation.

From the results of the experiments, Zachariasen deduced that the assumed isotropy in the shape and orientation of the domain is justified for both hambergite and α-quartz, since there was no systematic variation of r* with the orientation of the reflecting planes.

Zachariasen (1967) has also studied extinction in calcium fluoride. Here, he found that the applied extinction corrections were not sufficient to bring about a good agreement between the calculated and corrected structure factors and he assumed the differences were due to anomalous transmission (Borrmann, 1941).

Since this theory was published, many other tests, applications and extensions of the formulae have been undertaken. Extinction correction parameters have been introduced into many least squares refinement programmes, e.g. Larson (1969), and such parameters are often refined during the structure determination. There is no doubt that Zachariasen's work has led to a significant increase in interest in diffraction theory and accuracy of the structure factors.

Since the publication of the theory, however, many authors have cast doubts on the validity of the basic equations used and of the correctness of the mathematical derivations of the final formulae and have questioned the assumptions often used in its applications.

As stated before, when an x-ray beam is diffracted by a perfect crystal, a phase change of $\pi/2$ occurs during the scattering process. Any diffracted beam which is rescattered back into the main beam will therefore be out of phase with the main beam by π. How the main beam recombines with a many times scattered beam will depend on the number of times the beam has been scattered. The diffracted beam will also contain beams scattered many times. The intensity of the main beam and the diffracted beam can only be determined by taking into account these rescattering processes. In other words, the scattering process in a perfect crystal is a coherent process.

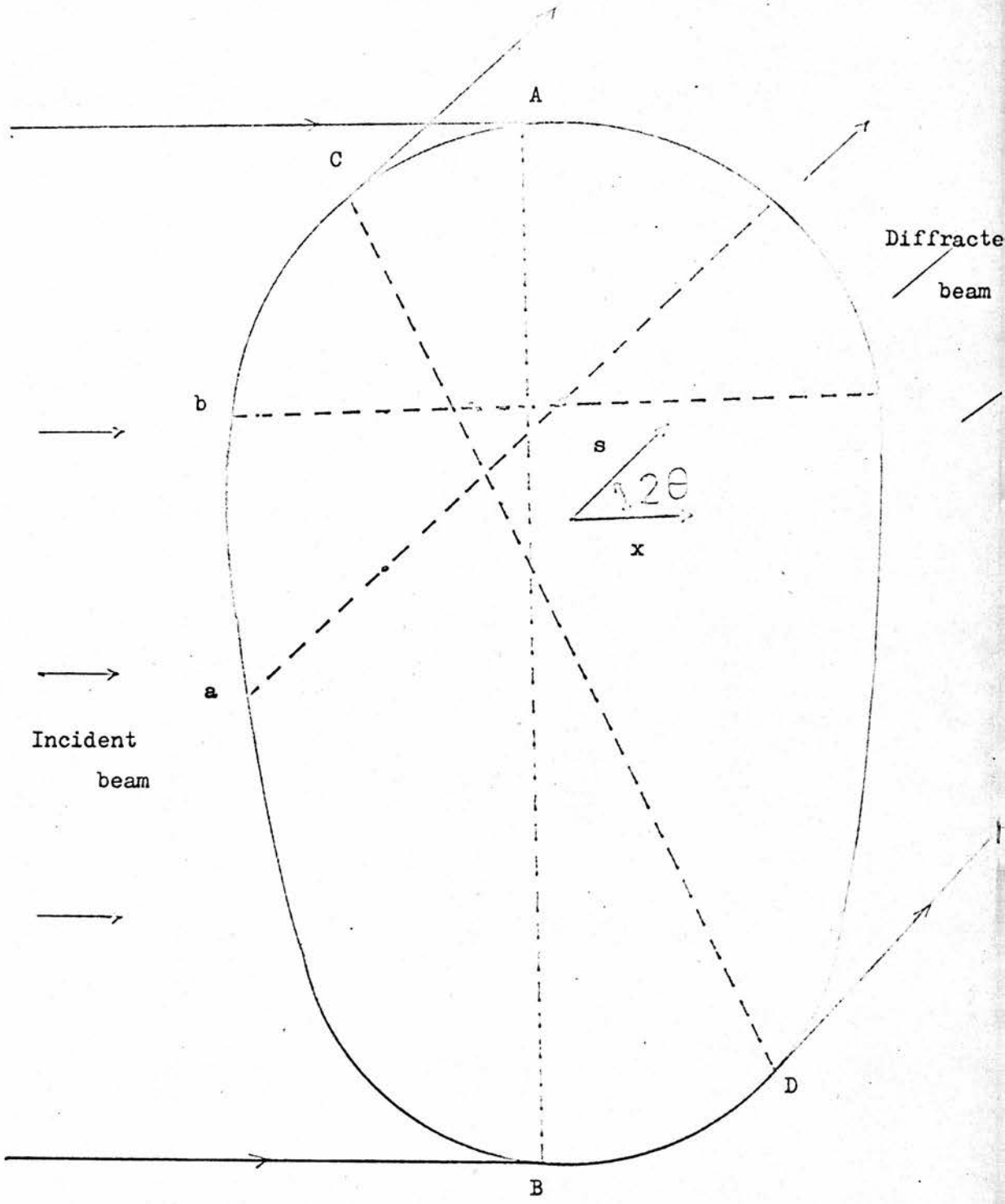

Fig. 8

Zachariasen's equations, however, are equations involving intensity only; the "feedback" term is added to the main beam as an intensity. Since the equations do not take coherence into account, it is unlikely that they will be able to correct for significant quantities of primary extinction. This was first pointed out by Werner (1969).

Another mathematical error, pointed out by Werner (1974) and Becker and Coppens (1974) relates to the coordinate system used by Zachariasen. Zachariasen's theory does not specify an origin of the direction of the incident and diffracted beams t_1 and t_2 respectively, fig. (5). Werner used a coordinate system where x specifies the direction of the incident beam and S specifies the direction of the diffracted beam, fig. (8). The relation between the two coordinate systems is:

$$t_1 = x - x_b$$
$$t_2 = S - S_a$$

where x_b and S_a are the equations of the boundary. Werner showed that the basic equations should be

$$\frac{\partial I_o}{\partial t_1} - \frac{\partial I_o}{\partial t_2}\,\frac{\partial S}{\partial x} = -\sigma I_o + \sigma I$$
$$\frac{\partial I}{\partial t_2} - \frac{\partial I}{\partial t_1}\,\frac{\partial x}{\partial S} = -\sigma I + \sigma I_o \ .$$

Comparison of these equations with those of Zachariasen (eq. 6), shows that the second terms on the left hand side of these equations were neglected by Zachariasen.

It is of interest to note that Brown and Fatemi (1973) also pointed out that the coordinate system used in Zachariasen's theory is an unusual one, does not have a unique origin, and the use of this coordinate system is not consistent with the basic differential equations. But they also noted that the use of a correct procedure changes very few of the results of Zachariasen because the error does

not affect most of the special cases treated and because Zachariasen selects his final form from several forms on the basis of their correspondence with experimental data.

For the primary extinction corrections, Werner suggested that the results of dynamical theory for slab geometry can be used as a reasonable approximation.

One very important limitation of Zachariasen's equations is introduced by defining the function $\phi(\sigma)$ as given in eq. (12). For a crystal of unknown shape, $\phi(\sigma)$ cannot be described by a single equation. In general, $\phi(\sigma)$ can be written as a polynomial in σt, the coefficients of which are functions of the shape of the crystal and the scattering angle. Zachariasen took this mosaic block to be a parallel plate diffracting in the symmetrical Bragg condition and he stated that it will be a good approximation for a sphere. However, since the mosaic block shapes of a real crystal are unknown and since the closed form of $\phi(\sigma)$ may not describe the angle dependence sufficiently, this approximation may be quite invalid in certain cases.

Cooper & Rouse (1969) investigated the problem of the angle dependence of the coefficients of the series for $\phi(\sigma)$ using a single crystal of Ca F_2 and neutron diffraction data which appeared to be suffering from severe extinction. They found marked angle dependence in the extinction coefficients for extinguished reflections and devised an empirical equation to give a better agreement between their calculated and corrected structure factors.

The shortcomings of Zachariasen's theory can be summarized as:

1. The basic equations do not express the flow of energy in a perfect crystal region, but they may be valid for real crystal case in the case of only secondary extinction.

2. Zachariasen's coordinate system does not have a unique origin, the coordinates used in the theory are only mutually independent if the crystal is a parallelopiped with faces parallel to the incident

and diffracted beams.

3. The approximations in eq. (12) and eq. (17) may not be valid in most of the cases.

4. The use of only a Gaussian distribution of the orientation of the mosaic blocks may not be valid.

5. Absorption effects cannot be treated separately from extinction unless extinction is small.

Becker & Coppens (1973) reconsidered the theory of extinction in a very similar way to Zachariasen's approach. They assumed that the basic transfer equations express the flow of energy inside a perfect crystal reasonably, using independent coordinates x_1 and x_2 based on an external coordinate system. Further, they pointed out that the reversal of the direction of the diffracted ray as was used by Zachariasen was wrong and one should use the true direction.

They solved the basic transfer equations obtaining the same solution for the function $\phi(\sigma)$ which was obtained by Zachariasen for the parallelopiped of fig. (6).

In the calculation of $\sigma(\varepsilon_1)$, the result of Becker & Coppens differs from the result of Zachariasen by the occurence of an additional term $\sin 2\theta$. The result for $\sigma(\varepsilon_1)$ is given as

$$\sigma(\varepsilon_1) = Q\, \nu^{-1} \int_{\nu} d\nu\alpha \, \frac{\sin^2 \pi\varepsilon_1\alpha}{(\pi\varepsilon_1\alpha)^2}$$

where $\alpha = \frac{\ell \sin 2\theta}{\lambda}$, ℓ being the thickness of the crystal parallel to the diffracted beam and the other symbols having their usual meaning.

This theory was applied to the parallel plate and spherical crystal cases. The result was in poor agreement with the result of dynamical theory in the parallel plate case. From this Coppens & Becker concluded that the basic transfer equations do not express the flow of energy inside a parallel plate shaped perfect crystal. The theory gave reasonable agreement with the 1st order approximation

results of dynamical theory in the case of spherical crystal. y_p was calculated by numerical integration over a gaussian grid and using the expression

$$y_p = \{1 + 2x + \frac{A(\theta)x^2}{1+B(\theta)x}\}^{-\frac{1}{2}}$$

the θ dependence $A(\theta)$ and $B(\theta)$ were found by means of least squares fit. The generalization of the theory for real crystal case was done in the same manner as Zachariasen, but because of the additional $\sin 2\theta$ dependence in $\sigma(\varepsilon_1)$, the type of the crystals defined by Zachariasen became less defined and it was suggested that crystal type varies with Bragg angle. On the other hand it was suggested that in type I crystals one should include the effect of primary extinction using the approximation:

$$y \cong y_p \cdot y_s$$

which has been used by various authors.

In the generalization of the theory for secondary extinction it is necessary to use the convoluted value $\bar{\sigma}$ instead of σ. In the calculation of $\bar{\sigma}$ Zachariasen used a Gaussian distribution function which governs the distribution of the orientation of the mosaic blocks, eq. (3). Coppens & Becker used both this function and a Lorentzian distribution which is given by

$$W_L = 2g/(1 + 4\pi^2 \varepsilon_1^2 g^2) \ .$$

From the comparison of the results and from the measurements using γ-ray resonance (Maier Leibnitz, 1972), they suggested that the actual distribution is more closely Lorentzian than Gaussain.

As described before in his theory, Zachariasen states that primary extinction will be generally negligible for the large structure factors when the block size is less than 10^{-4} cm and secondary extinction will be dominant and this is the case for most of the experiments.

However, in some of the experiments, the block sizes deduced from various materials were greater than 10^{-4} cm implying primary extinction is taking part, e.g. hambergite (Zachariasen, 1968), calcium fluoride (Zachariasen, 1968).

Denne (1972), using α-glycine crystals of different sizes showed that the amount of extinction in these crystals was independent of their shape and size, suggesting primary extinction is dominant.

Lawrence (1972, 1973), investigated extinction on large parallel plates of lithium fluoride and magnesium oxide whose cross-sectional areas were much larger than that of the incident beam. It was noted that the intensities of symmetry equivalent reflections, after the application of transmission factors which take into account absorption and the different volumes of the crystal irradiated, were the same, regardless of the path length through the crystal, implying that the extinction was of the primary type. Therefore, only one mosaic block was diffracting a parallel monochromatic beam at one time. Using Zachariasen's primary extinction correction, a mosaic block size of 3×10^{-3} cm was deduced for lithium fluoride which corresponds to a dislocation density of 10^{5} cm^{-2} which well agreed with the value given by manufacturers of the material. For MgO, Lawrence deduced a mosaic block size of 3.56×10^{-3} cm which is again far larger than the minimum size of block required to ensure that only primary extinction was taking place.

Killean, Lawrence and Sharma (1972) investigated extinction using a small spherical LiF crystal which was from the same batch of material as used by Lawrence. Assuming only secondary extinction, a mean radius of mosaic block of 1.5×10^{-6} cm was obtained. Comparing this value with the value obtained from a strain equation and the value obtained by Lawrence, it was deduced that Zachariasen's procedure gave a physically unreasonable value for r^{*}.

As stated before, primary extinction is a coherent process and in secondary extinction no coherence is assumed between the rays diffracted from various macroscopic regions of the crystal. As can be seen from eqs. (18) and (27) the mathematical form of the primary and secondary extinction corrections are very similar. If a particular data set which was affected by extinction was corrected assuming only primary extinction, a mosaic block size r_p would be obtained where

$$r_p^2 = \frac{2x}{3A}$$

where A is a constant for a particular reflection. If the data set was then corrected assuming secondary extinction (type II crystal), a mosaic block size r_s would be obtained where

$$r_s = \frac{x}{A\bar{T}} .$$

Due to the similarity of eqs. (18) and (27), the correction would be equally applicable for both types of extinction and the mosaic block sizes would be approximately related by

$$r_p^2 = (\frac{2}{3})\bar{T}\, r_s .$$

According to this relation, if a block size of 10^{-4} cm is obtained assuming secondary extinction only, for a crystal of $\bar{T}$ = 0.02 cm a block size of 2×10^{-3} cm would be obtained assuming primary extinction only. Therefore, in this case, the block size deduced cannot be used as a justification of the assumption that only secondary extinction is taking part. Identification of the type of extinction can only be done by testing the variation of extinction with path length, Lawrence (1974).

CHAPTER 2

Introduction:

Although Zachariasen's equations have been generally applied in many cases, doubts still exist as to their validity. These doubts can only be resolved experimentally and there still remain two fundamental questions regarding the applicability of the equations. These questions are:

1) Is it possible experimentally to differentiate between the two types of extinction, primary and secondary?

2) Do Zachariasen's equationsyield physically significan parameters?

In an attempt to answer these questions, a study of the large crystals of D(+) tartaric acid was undertaken. An attempt was made to determine the type of extinction present and to investigate the physical parameters obtained from the application of Zachariasen's equations.

An intensity measurment project to test the accuracy of structure factors measured by different laboratories had been designed by the International Union of Crystallography, (Abrahams, Hamilton and Mathieson, 1970). In this project, seventeen sets of measurments of structure factors of D(+) tartaric acid, within the range $(\frac{\sin\theta}{\lambda}) < 0.5$ Å^{-1}, were provided by the participants. Each participant used

a different crystal, all being derived from a single crystallization batch. In the report of the project, all data had been put on the same scale by the method of Hamilton, Rollett and Sparks (1965), and the differences between the sets in relation to a number of variables, such as intensity, Braggangle, indices of reflections, were examined and the report arrived at certain general conclusions.

Later, Mackenzie (1974) reduced theapriori assumptions to a minimum, worked out the differences between sets of structure factors again, and came to the following conclusions-

1) There were systematic structure factor dependent differences in the structure factors derived from different single crystals. These differences were beginning to be apparent at medium values of structure factors and were increasing to be about 15% of the structure factor for the largest structure factors.

2) These differences were not due to improper scaling or other errors in data reduction and the angle dependence of these differences was minor.

3) The differences were probably wavelength dependent but there was not enough data to check this.

4) They were not due to differences between the apparatus or measuring techniques used.

It was therefore concluded that the differences were consistent with extinction. The very large variation in the intensities obtained by different participants emphesised the importance of extinction in the measurment of accurate structure factors and, in view of the results obtained in the project, it was decided that D(+) tartaric

acid would be an excellent material on which to investigate extinction.

Recent investigations into extinction in many materials have been carried out e.g. hambergite, α-quartz, lithium fluoride, calciumfluoride (Zachariasen 1968a, 1968b,1968c), calciumfluoride (Cooper, 1970), bariumfluoride (Cooper, Rouse and Willis, 1968), strontiumfluoride and calcium fluoride (Cooper and Rouse, 1971) and many other materials. In these studies, the integrated intensities were measured from small crystals, completely bathed in the X-ray beam, and a least squares routine which included extinction parameter as an additional parameter, was applied to the data. This method was thought to be unsatisfactory for the following reasons:

1) With small crystals, it is not usually possible to test the variation of extinction with pathlength satisfactorily. The variation of the pathlengths of different reflections is usually quite small unless one of the dimensions is large. Without a test of the variation of extinction with path length, primary and secondary extinction cannot be distinguished.

2. If the crystal is of irregular shape, absorption corrections cannot be accurately applied.

3) The use of a least-squares routine implies an established mathematical relationship between extinction and intensity. Since the experiments are being done to establish this relationship, some other method of analysis should be used.

The first experimental observations on extinction were carried out on large plates of sodium chloride,

(Bragg, James and Bosanquet, 1921). The object of these experiments was to find accurate structure factors from rocksalt and to check the intensity formulae which were suggested by Darwin (1914). Large parallel plates of sodium chloride of various thicknesses with cross-sectional areas larger than the incident X-ray beam were used in the experiments. Accurate intensity measurments were obtained and absorption corrections applied. Extinction was regarded as an increase in the effective absorption coefficient and, analysing the variation of absorption coefficient with the thickness of the crystals, extinction coefficients were obtained for strong reflections. It was assumed that the integrated intensity, R, for a reflection was given by

$$R = QT\, e^{-(\mu+gQ)T}$$

where Q is the reflectivity and T is the pathlength of the rays through the crystal. As can be seen, the normal absorption coefficient has been replaced by an effective absorption coefficient, μ', given by

$$\mu' = \mu + gQ$$

and it was found that the amount of extinction was proportional to the reflectivity. By repeating the measurments for different thicknesses and for different degrees of perfection (which was obtained by different amounts of grinding) of the crystals, the variation of extinction with thickness and perfection was investigated.

The use of large crystals of regular shape having a cross-sectional area larger than the X-ray beam has the following advantages:

1) The variation of extinction with pathlength

through the crystal can be adequately investigated and this is the only way to determine the type of extinction i.e. whether it is primary or secondary, e.g. Lawrence (1972, 1973).

2) Absorption corrections are exact apart from any errors in the absorption coefficient μ. In the case of small, arbitrary shapes, it is very difficult to measure precisely the dimensions of the crystals which are very important in the calculation of the corrections. The usual way is to evaluate absorption integrals approximately, using numerical methods for the arbitrary shapes, which may contain significant errors in most of the cases. In large plate shape crystals one does not need to deal with these complications. Absorption corrections are given by simple formulae and as long as the thickness of the crystal is known accurately, absorption corrections can be calculated in a straight forward manner.

3) The results are not dependent on the uniformity of the incident beam.

4) Intensities can be measured on any conventional diffractometer and, since the diffracted intensities are much larger compared to the diffracted intensities from small crystals, the accuracy in measurment is greater.

5) Grinding the crystals to special small shapes can affect the perfection of the crystals in an irregular manner.

An attempt was therefore made to grow large, parallel-plate shaped crystals of D(+) tartaric acid having uniform thickness.

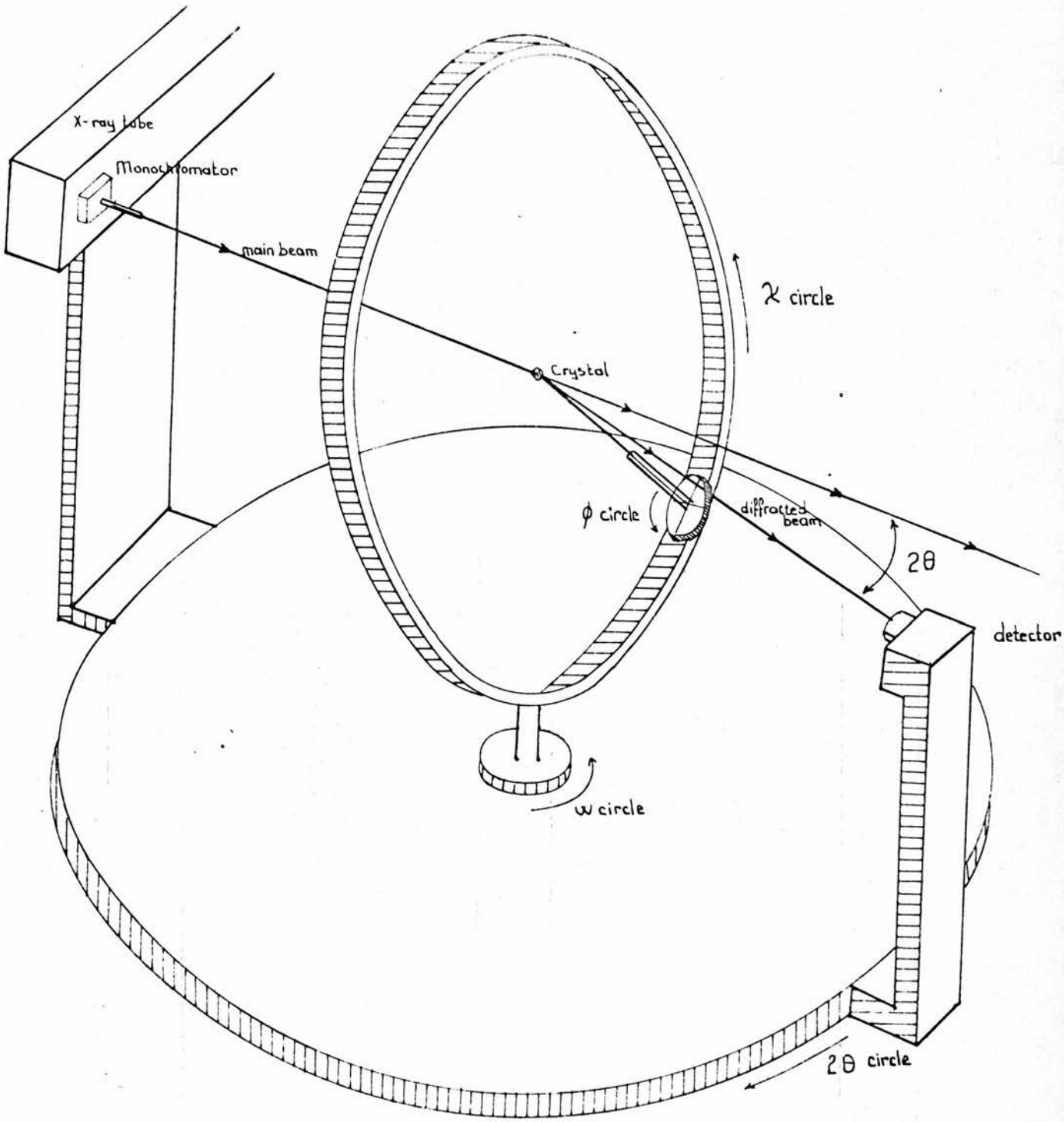

Fig. 9

Schematic diagram of 4-circle diffractomer

Growth of the crystals:

In order to obtain large, plate shaped D(+) tartaric acid crystals different solutions were tried and the best results were obtained from an aqueous solution. Crystals of D(+) tartaric acid were grown from saturated aqueous solutions by evaporation and many crystals of various thickness with a large cross-sectional area compared to X-ray beam and which were considerably more uniform than the others were chosen.

From the oscillation photographs and measurments by microscope it was found that all of the crystals were grown in the same way having thicknesses between 0.2 mm to 0.5 mm along the a axis.

Apparatus:

Quantitative intensity measurments were carried out on a Siemens four-circle diffractometer which has four setting circles, ϕ, χ, w and 2θ circles. w and 2θ circles are coupled together with a ratio 1:2, reducing the number of setting circles to three. This diffractometer has a quarter χ circle, fig (9). The detector is controlled by 2θ circle which is mounted such that it lies in the equatorial plane. The crystal is mounted on to a shaft perpendicular to this plane with an adjustable goniometer head, whose rotation is controlled by the ϕ circle.

The apparatus has a normal beam equatorial geometry, both the incident and diffracted beams lying on the equatorial plane. In order to bring any reflection(hkl) into diffracting position, the reciprocal lattice point should be moved to a corresponding point on the Ewald sphere by ϕ rotation and then this point can be moved to the equatorial plane by χ rotation.

ϕ, χ, and W circles aredriven by three stepping motors, step size is 0.01°, and this corresponds to a 0.02° step size on 2θ circle. Settings are checked by means of digitizer drums.

The diffracted intensity is received by a scintillation counter. In order to prevent lost counts in the case of large intensities which can exceed the capacity of the counter, an attenuator system is placed in the path of the main beam. This system consists of a disc, attached to the X-ray tube, which can revolve around its axis. This disc has six holes, five of them containing different attenuators for the progressive attenuation of the main beam. In the path of the main beam there is also a second disc containing the $K\beta$ filter and the shutter. In the experiments the beam was monochromatised by a graphite monochromator.

The coupling of W and 2θ circles together with the ratio 1:2 is called "moving crystal - moving detector scan" or "$\theta-2\theta$" scan. During the experiments this scan was employed. In this method, as crystal rotates through an angle $(\theta-\Delta\theta)$ to $(\theta+\Delta\theta)$ about the exact Bragg angle, the detector moves through an angle $(2\theta-2\Delta\theta)$ to $(2\theta+2\Delta\theta)$.

All of the input and output channels of the Siemens four-circle diffractometer are connected to an IBM-1130 computer with an interface and it is controlled by this computer executing automatic data collection programs. The programs are stored in core image on the computer disc.

Data collection programmes:

DSET4:

The programme DSET4 is mainly used to facilitate the crystal setting. Using this programme, many operations which are required for automatic data collection can be performed singly, .e.g. setting the circles to their zero positions, setting the circles to a given angle, inserting any of the six attenuators in the path of the main beam, determination of the orientation matrix, measuring the integrated intensity of a given reflection. Each one of these operations can be called using the switches on the keyboard of the computer in any sequence.

One of the most important functions of DSET4 is the determination of orientation matrix. Orientation matrix is the relation between the original position of the crystal on the diffractometer and the diffracting positions. In automatic data collection, the ϕ, χ, and θ values for a certain reflection are calculated from the orientation matrix. DSET4 contains two versions of orientation matrix determination. In one of them, orientation matrix is determined from the manual determination of the ϕ, χ and θ values of any three non co-planar reflections while in the other one, orientation matrix is determined using the ϕ and χ values of only two non co-linear reflections and the cell parameters. After orientation matrix determination ϕ, χ and θ values for any reflection and the reciprocal and the real cell parameters can be extracted.

Using DSET4, the measurment of integrated intensities can also be done for any of the reflections. A five-point measurment cycle, which will be described later, is used

in the measurments of integrated intensities. The only difference under DSET4 is the step size and time required for each step is not flexible and has to be given as input data initially. It is also possible to obtain line profiles for any of the reflections.

DIFF8:

Programme DIFF8 controls the diffractometer during automatic data collection. In this programme from the orientation matrix, from the information about the segments of reciprocal space to be measured from the minimum and maximum values of 2θ required, from the order in which the indices are to be taken and from the specification of systematic absences, reciprocal space is explored in a systematic manner. The ϕ, χ and θ circles are driven automatically to the angles calculated from orientation matrix which is given as input data. By counting for 0.5 sec. at the peak of the reflection with the thickest attenuator in use, the correct attenuator setting is made, in order to make sure that the maximum counting rate of the detector is not exceeded, so lost counts are prevented. If the maximum count rate is exceeded the measurment will be done the thickest attenuator in use, but this will be indicated in the output data. In these reflections lost count corrections will be necessary.

The integrated intensities are measured using a five-point measurment cycle about the exact Bragg angle. The range of scan is

$$(\pm\Delta\theta) = P + Q \tan\theta$$

where P and Q are specified in the input data. The scan is in steps of 0.01°. Counting time for steps is related to the counting statistics and accuracy of measurment. Calculation of the time per step is as follows:

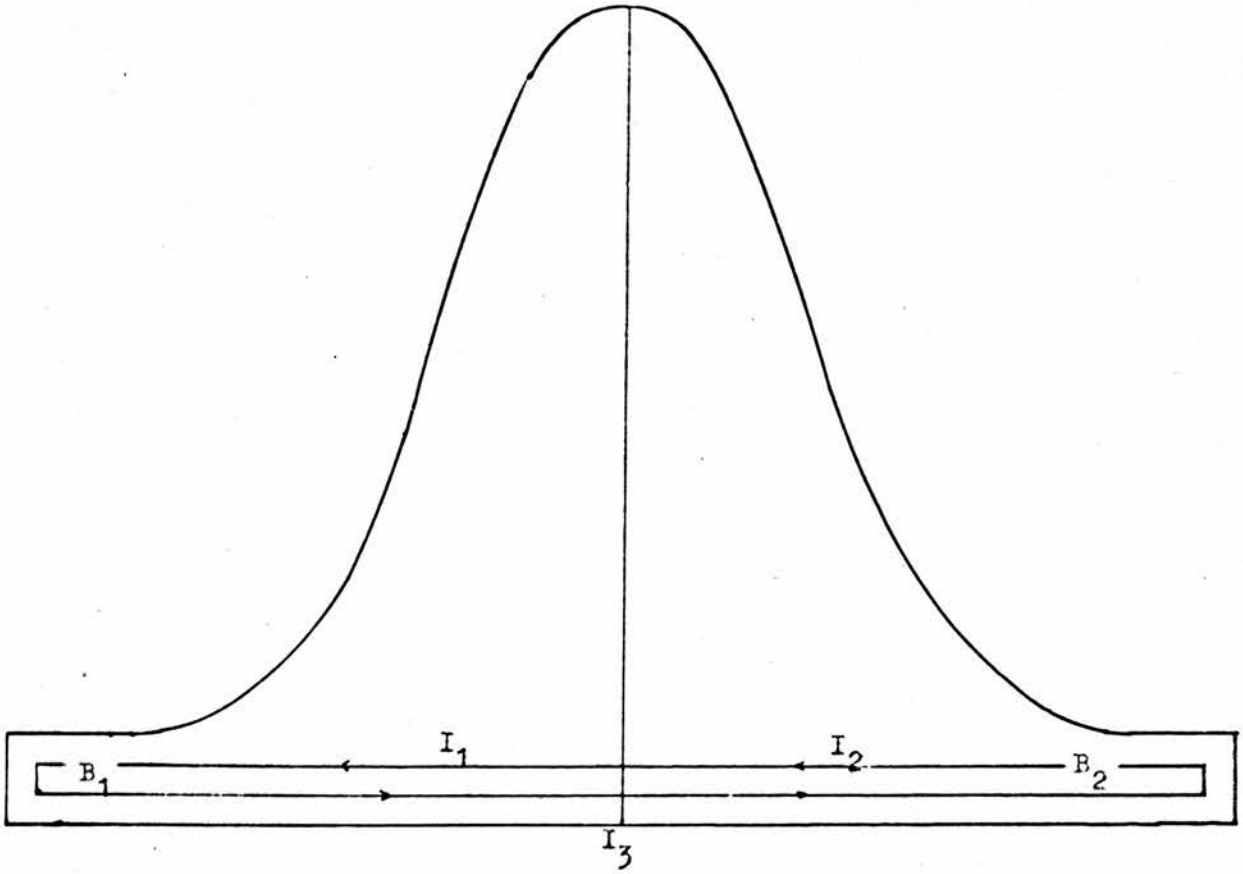

Fig. 10 Five-point measuring scan

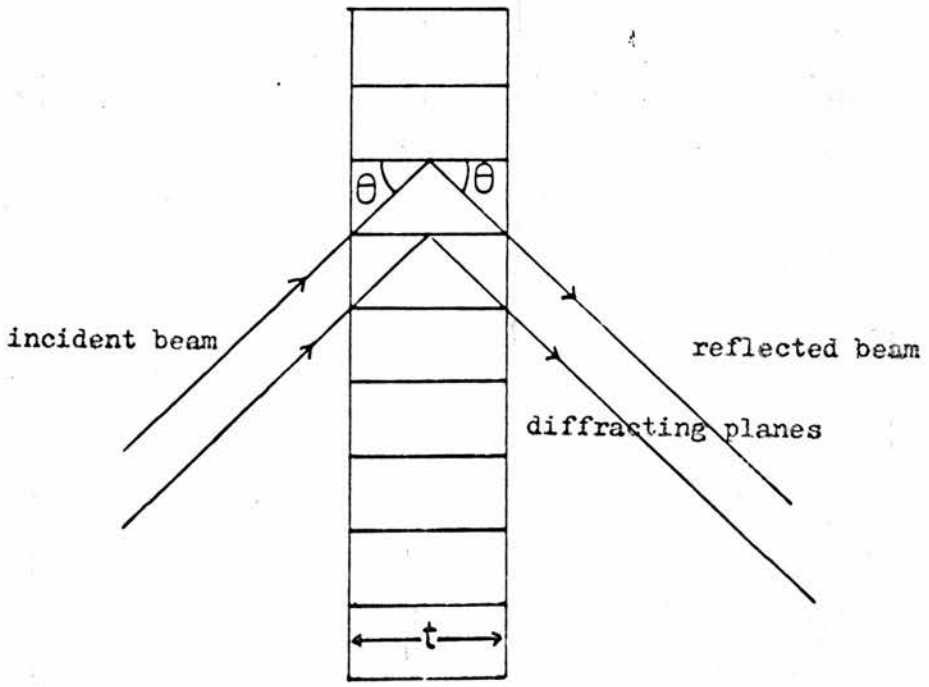

Fig. 11 Symmetrical Laue reflection

A trial time per step q, a maximum time Tm per step, a pre-stated percentage accuracy p and a percentage accuracy Pc for the weak reflection criterion are specified in the input data. Times are expressed as integers, where integer 1 corresponds to 5.4×10^{-3} sec. First, the reflection is measured using the trial time per step q and a time per step T is calculated ensuring the required accuracy p. If T is less than Tm, the reflection is then measured using this time per step. If T is greater than Tm, an accuracy p' for the reflection is calculated if it to be measured for Tm. If p' is less than the weak reflection criterion Pc, the reflection is measured using Tm as time per step. If p_c is less than P' then reflection is not measured and is considered to be absent.

Then, in five-point measurement cycle (fig. 10), the detector measures the half peak I_1, measures the background B_1 then measures the full peak I_3, then measures again background B_2 and half peak I_2 in steps of 0.01°, using the range and time per step described above. The time spent for measuring the background counts is half the time for measuring the peak. Therefore the integrated intensity for the reflections on the same scale will be given by

$$I = [(I_1 + I_2 + I_3) - 2(B_1 + B_2)] \times \frac{\gamma}{T}$$

where γ is the attenuator factor and T is time per step.

In using DIFF8, repeating the measurments of some standard reflections after each set of n reflections where n is specified in the input data, it is possible to check the overall stability of the system.

Data Collection:

Data was collected for all seven crystals using CuKα radiation and, for four of them, data collection was repeated using MoKα radiation.

Experimental Conditions for CuKα data:

Applied voltage	= 35 KV
Current	= 20 mA
Trial time per step	= 0.54×10^{-2} sec.
Maximum time per step	= 0.54 sec.
Percentage accuracy	= 2%
Weak reflection accuracy	= 20%

For MoKα data applied voltage was 40 KV and the current was 18 mA and the other conditions were the same as in CuKα data.

The crystals were first set on goniometer heads using glass fibres. Oscillation photographs ensured that all of them have b axis as the oscillation axis. By taking oscillation photographs successively, the required corrections were done in the setting of the crystals on the goniometer heads.

When the automatic data collection was being carried out for the first crystal, it was noticed that the backgrounds and halfpeaks on both sides of the diffraction peaks were highly asymmetric. It was concluded that the diffraction peaks were not centered because of a fault in diffractometer circles. The scan was covering the whole peak, therefore it was possible to measure the integrated intensities, but because the peaks were not centered, automatic setting of attenuators in some of the reflections were incorrect, leading to lost counts. It

was decided to centre the peaks manually and to carry out integrated intensity measurments using the programme DSET4 instead of automatic data collection programme DIFF8.

Using CuKα radiation, for all seven crystals, data was collected by centering the diffraction peaks manually. All of the integrated intensities of(0kl) and(0$\bar{k}$l) reflections were measured up to a θ value of 70° using the programme DSET4.

During the data collection using MoKα radiation, the automatic data collection programme DIFF8 was employed, the fault in the diffractometer arcs having been corrected. The checks on the diffraction peak shapes showed that the peaks were symmetric and properly centered. For four of the crystals, for the same reflections as in the CuKα data collection, the integrated intensities were measured.

Data reduction:

The attenuation factors were measured in a seperate experiment. In this experiment, one weak and one strong reflection having the attenuator 1 and attenuator 3 respectively during the data collection, were chosen. Using a long time per step the integrated intensities were measured, setting attenuators 1,2,3,4 for the weak reflection. From the ratios of these integrated intensities to the integrated intensiies obtained using attenuator 1, attenuation coefficient were found as

1:2.062:4.0189:7628:25.877:36.837

These attenuation coefficients were applied to the raw data.

The square of the observed structure factors, $|Fo|^2$, were obtained from the integrated intensities, R, from the equation

$$R = c|Fo|^2 A (Lp)^{-1}$$

where A is the absorption correction and $(Lp)^{-1}$ is the Lorentz polarization correction.

All of the reflectionsused were symmetrical Laue reflections i.e. the diffracted beam emmerged from the crystal at the opposite face from the incident beam and all path lengths through the crystal were the same for each reflection, (Fig.11). For this geometry the absorption factors are given as

$$A = (t/\cos\theta)\exp(-\mu t/\cos\theta)$$

where μ is the absorption coefficient and t is the thickness of the crystal.

To apply the absorption corrections one needs to know the thickness of the crystals accurately. The measurements of the thicknesses of the crystals were difficult and a method of measuring t was therefore devised. In this method crystals were placed normal to the incident beam and the transmitted intensities I through the crystal were measured. The incident intensities Io with crystal removed were also measured in each case to eliminate the possibility of long term variations in the incident beam intensity. Then the values of μt were calculated from

$$\mu t = \ln(Io/I)$$

The value of μ was determined from the International Tables of Crystallography vol IV (1974).

For CuKα radiation $= 14.82\ cm^{-1}$

For MoKα radiation $= 1.619\ cm^{-1}$

Even with the thick attenuator in use, the intensities were very large in these measurments. Therefore a copper foil was introduced in front of the detector aperture in order to prevent lost counts. Measurments were carried out

using CuKα radiation for all of the crystals. For four of them again, the measurments were repeated using MoKα radiation. In order to get rid of the ($\lambda/2$) radiation, the power of the X-ray tube was cut down reducing the applied voltage to 34 KV which does not excite ($\lambda/2$) radiation for MoKα radiation. This was not possible in the case of CuKα radiation.

For six of the crystals, the thicknesses obtained using CuKα radiation were

for Crystal 1 : $t_1 = 0.0455$ cm
for Crystal 2 : $t_2 = 0.0406$ cm
for Crystal 3 : $t_3 = 0.023$ cm
for Crystal 4 : $t_4 = 0.0217$ cm
for Crystal 5 : $t_5 = 0.0204$ cm
and for Crystal 6 : $t_6 = 0.01923$ cm

In the same way, using MoKα radiation the thicknesses obtained were:

for Crystal 1 : $t_1 = 0.0458$ cm
for Crystal 2 : $t_2 = 0.04028$ cm
for Crystal 4 : $t_4 = 0.0223$ cm
and for Crystal 5 : $t_5 = 0.01966$ cm

After the comparison of above results with each other and with the values measured through the telescope of the diffractometer, thicknesses of the crystals were taken as:

$t_1 = 0.046$ cm
$t_2 = 0.040$ cm
$t_3 = 0.023$ cm
$t_4 = 0.022$ cm
$t_5 = 0.0197$ cm
$t_6 = 0.0192$ cm

with a maximum percentage error of 3% on each.

Using these values, the transmission factors were calculated for each reflection and the absorption corrections were applied to the raw data for all of the crystals.

The structure of D(+) tartaric acid had been refined by Okaya and Stemple (1966) and although the calculated structure factors may not have been correct because ofextinction in

the observed data and possible inaccuracies in the least- squares process , it was assumed that they were approximately on an absolute scale.

On the other hand, it was thought that, if the average value of the structure factors obtained in different experiments using MoKα radiation, in the project of International Union of Crystallography is taken, it will provide a better set of structure factors since the data will be less affected by extinction. Therefore it was decided to scale these average values of structure factors to those refined by Okaya and Stemple and then to scale the raw data to these structure factors which are now assumed to be on an absolute scale. Scale factors were found using small structure factors which may be affected by small extinction only and the data sets were put into absolute scale applying these scale factors.

After these corrections and scaling, the symmetry equivalent reflections were compared in each set, calculating the reliability factors between $(0kl)$ and $(0\bar{k}l)$ sets. Reliability factor for the nth data set was

$$R_n = \Sigma(|F_{(0kl)}|^2 - |F_{(0\bar{k}l)}|^2) / \Sigma |F_{(0kl)}|^2$$

In one of the seven crystals, the differences between symmetry equivalents were large in most of the reflections, suggesting that this crystal was not uniform. This data set was therefore rejected. The differences between the symmetry equivalents were large in the (002) and (011) reflections in all of the crystals. These reflections were omitted from the data. Apart from these, the reliability factor R_n were

	← $F^2_{ob.}$ (CuK$_\alpha$) →						← $F^2_{ob.}$ (MoK$_\alpha$) →				
hkl	crys1	crys2	crys3	crys4	crys5	crys6	crys1	crys2	crys4	crys5	F^2_k
001	0.8	1.	0.8	0.71	0.91	0.84	2.3	2.3	2.3	1.76	0.76
002	163.6	218.2	197.5	261.3	345.2	261.2	637.9	538.5	701.9	787.8	911.2
003	9.3	9.5	9.	9.9	11.	10.4	11.7	11.6	11.7	11.4	12.3
004	172.	226.6	206.8	228.8	265.1	249.7	400.9	379.3	412.6	427.	439
005	9.6	9.8	9.6	9.7	9.6	9.	11.6	11.6	11.3	11.7	11.2
006	32.5	32.4	33.4	33.9	35.3	36.6	39.5	39.5	39.9	40.1	40.3
012	60.7	66.5	70.2	71.2	78.6	78.9	101.5	97.8	101.5	104.6	108.3
013	134.6	164.1	169.	175.4	204.	202.3	275.3	263.	280.4	291.3	310.1
014	18.	18.3	18.1	18.4	19.	20.6	22.9	22.7	22.8	23.	22.8
015	22.9	23.2	23.3	23.	24.2	26.5	28.	28.3	28.7	28.5	29.4
016	31.6	33.8	33.4	36.	33.8	35.4	37.4	38.5	38.2	38.	38.2
021	25.8	27.1	28.	28.8	29.3	32.	38.3	37.7	37.2	37.7	34.6
022	13.7	13.5	13.6	13.7	13.9	15.4	17.6	17.	17.3	17.4	24.1
023	108.8	129.6	138.7	132.7	150.9	149.1	193.4	188.8	193.2	199.3	188.2
024	72.7	79.3	82.2	79.7	86.9	91.4	109.	108.4	109.3	110.4	114.6
025	20.2	20.9	21.2	21.3	21.4	22.	24.9	25.1	24.9	25.3	26.8
031	166.	195.	226.3	209.6	236.1	244.6	330.5	330.7	347.6	350.2	364.4
032	33.1	34.5	35.	35.6	36.2	40.2	46.9	46.4	45.9	46.	46.2
033	58.8	65.8	67.9	65.5	70.8	76.4	91.8	89.	88.8	90.3	90.5
034	11.6	11.6	11.9	12.	12.	13.2	14.4	14.2	13.9	14.2	13.
035	3.5	4.	3.9	4.	3.7	4.	4.	4.	4.1	4.	3.5
041	26.8	27.7	27.1	27.7	27.8	31.2	37.5	37.9	37.4	36.9	37.9
042	15.2	13.6	13.6	14.2	13.6	16.	18.1	17.7	17.8	18.	20.
043	29.1	30.	30.9	31.5	32.2	34.7	38.3	38.2	37.8	38.8	38.3
044	51.4	56.1	59.4	58.6	59.6	63.7	76.6	74.8	74.4	75.5	76.8
051	140.4	157.7	165.9	163.8	173.9	182.9	247.	257.4	255.2	255.3	266.3
052	13.9	14.	14.3	14.8	14.2	16.1	17.6	17.4	18.4	17.9	19.2
053	49.4	54.9	55.6	54.5	56.7	59.	72.7	71.8	70.7	72.	73.8

Table 1

For CuKα radiation:

$R_1 = 0.0247$
$R_2 = 0.0544$
$R_3 = 0.0248$
$R_4 = 0.0384$
$R_5 = 0.0323$
$R_6 = 0.0726$

And for MoKα radiation

$R_1 = 0.0247$
$R_2 = 0.0603$
$R_4 = 0.0417$
$R_5 = 0.0311$

These values were thought to be satisfactory in view of the 2% counting statistic accuracy. The $|Fob|^2$ values of the symmetry equivalent reflections were averaged and, therefore, the $|Fob|^2$ values of okl reflections for six crystals of different thicknesses, using CuKα radiation for all of them and using MoKα radiation for four of them, were obtained. These values are shown in table (1).

To compare the consistency of the experiments the R_{ij} values were calculated between the sets of data, for small intensities only, since these reflections will have small extinction.

The R_{ij} values for intensities are given by;

$$R_{ij} = \sum||F_i|^2 - |F_j|^2| / \sum|F_i|^2$$

From this R_{1j} values were obtained for CuKα sets as:

$R_{12} = 0.0274$
$R_{13} = 0.0399$
$R_{14} = 0.0420$
$R_{15} = 0.0530$
$R_{16} = 0.0964$

The R_{1j} values increase slightly with decreasing thicknesses of the crystal, suggesting that, although the intensities used in the calculation of R_{1j} were low, there was still a thickness dependent effect which could have been caused by secondary extinction, even at these low intensities.

The R_{ij} values obtained for MoKα sets were smaller;

$$R_{12} = 0.0163$$
$$R_{14} = 0.0302$$
$$R_{15} = 0.0243$$

Any thickness dependence is not detectable but when compared to the R_{1j} values in CuKα case, it strongly suggests that the differences between the sets of data are wave length dependent. The R_{1j} values obtained were thought to be reasonable. With an average 2% error in |Fob|, the data sets were consistent with each other.

Inspection of the scaled data showed that, at least for CuKα radiation, the strong reflections seemed to be fairly strongly extinguished. Investigation was carried out to determine the following points:

1) How did the thickness of the crystal affect the amount of extinction?

2) Was it possible to determine whether the extinction was secondary or primary?

3) Could a mathematical equation describing extinction be found?

In the investigation, Zachariasen's procedure was initially assumed to be valid, that is;

$$y = (F_{ob}/F_k)^2 = (1 + 2x)^{-1/2}$$

where Fk is the kinematic structure factor. The average values of the observed values of the structure factor |Fob|, of the MoKα data, which was obtained from the International Union of Crystallography project and had been put into an approximate absolute scale, were taken as Fk values. Assuming only secondary extinction, for intermediate type x is given by eq. (30), for type I x is given by

$$x = gQ\bar{T} , \qquad (34)$$

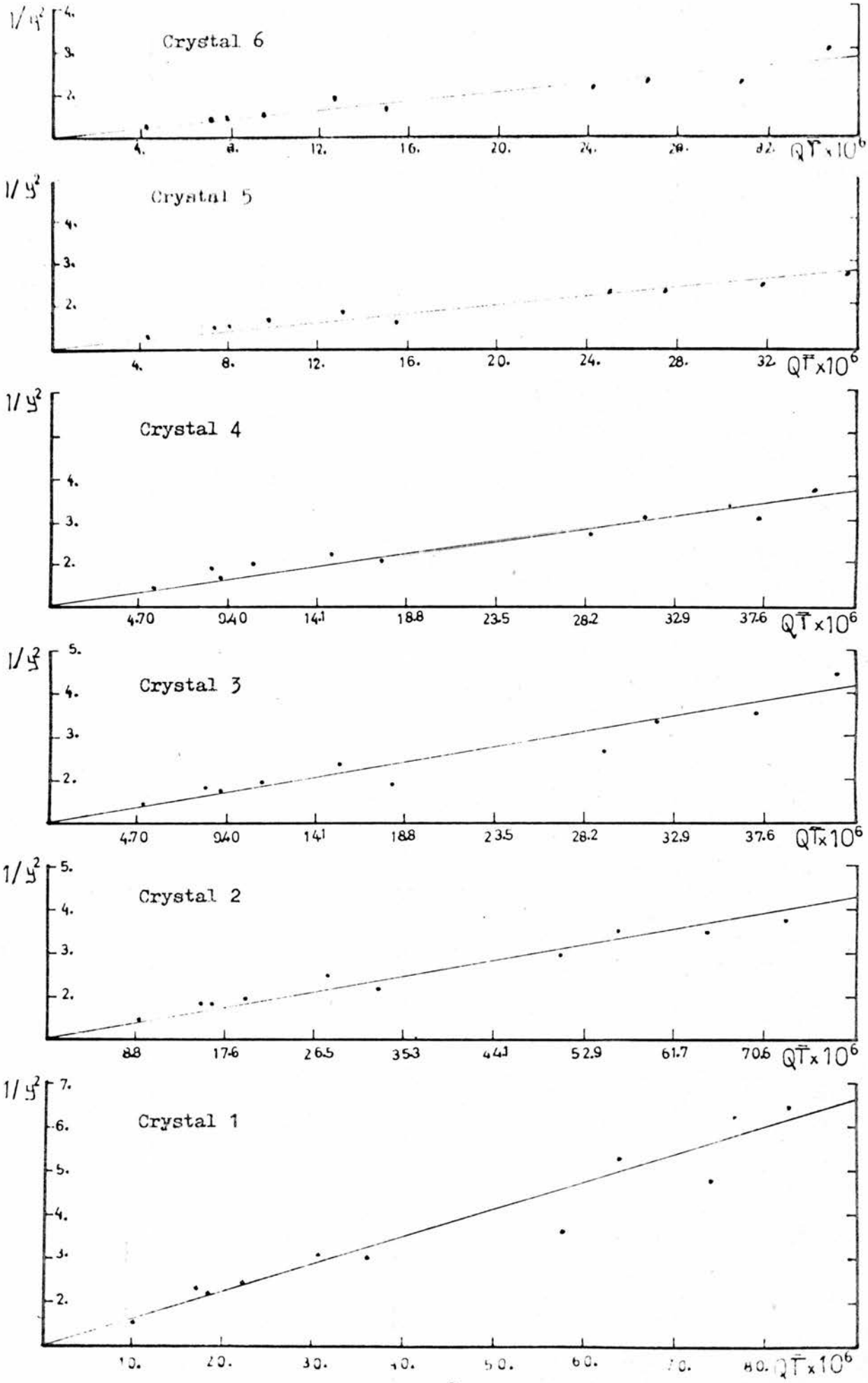

Fig. 12 Graphs of $Q\bar{T}$ against y^{-2} for Cu radiation

h k l	Q x 10^6	crystal 1		crystal 2		crystal3		crystal 4		crystal 5		crystal 6	
		$1/y^2$	$Q\bar{T}$	$1/y^2$	$Q\bar{T}$	$1/y^2$	$Q\bar{T}$	$1/y^2$	$Q\bar{T}$	$1/y^2$	$Q\bar{T}$	$1/y^2$	$Q\bar{T}$
0 0 4	1557.8	6.51	82.5	3.75	72.6	4.50	41.5	3.68	40.2	2.74	35.5	3.09	34.6
0 3 1	1477.9	4.81	74.0	3.49	65.1	4.40	37.2	3.02	36.0	2.38	31.8	2.22	31.0
0 1 3	1277.1	5.30	63.8	3.57	56.1	3.36	32.0	3.12	31.0	2.31	27.4	2.35	26.7
0 5 1	954.9	3.60	57.9	2.85	50.9	2.57	29.0	2.64	28.2	2.34	24.9	2.12	24.2
0 2 3	699.4	2.99	36.0	2.11	31.6	1.84	18.0	2.01	17.5	1.56	15.5	1.59	15.1
0 1 2	636.8	3.18	30.4	2.65	26.7	2.38	15.3	2.31	14.8	1.90	13.1	1.88	12.7
0 2 4	400.2	2.48	22.2	2.08	19.5	1.94	11.1	2.07	10.8	1.73	9.5	1.57	9.3
0 4 4	278.0	2.23	18.3	1.87	16.1	1.67	9.2	1.71	8.9	1.66	7.9	1.45	7.7
0 3 3	316.3	2.36	17.2	1.88	15.1	1.77	8.6	1.90	8.4	1.63	7.4	1.40	7.2
0 0 6	144.6	1.53	10.1	1.54	8.9	1.45	5.1	1.41	4.9	1.30	4.3	1.21	4.2

Table 2

and, for type II,

$$x = \lambda^{-1} . rQ\bar{T} \qquad (35)$$

Assuming only primary extinction, x is given by

$$x = (3/2)(r^2/\lambda)\, Q \qquad (36)$$

For secondary extinction, since

$$(1/y)^2 = 1 + 2x ,$$

$(-\frac{1}{y})^2$ will be linearly dependent on $(Q\bar{T})$, while for primary extinction, it will be linearly dependent only on Q and there will be no dependence on $\bar{T}$.

For all of the data sets the $(1/y)^2$ values were calculated from

$$(1/y)^2 = (F_k/F_{ob})^4$$

CuKα data:

The Q, $Q\bar{T}$ and $\frac{1}{y^2}$ values of the ten most extinguished reflections are shown in Table (2)

(a) Assuming only secondary extinction:

For each crystal, the values of $(1/y)^2$ were plotted against $Q\bar{T}$. These are shown in fig. (12). It can be seen that there are significant departures from linearity but the pattern of the points was very similar for each graph. If, strictly following Zachariasen's theory, a straight line is drawn passing though the origin ($1/y^2 = 1$) and best fitting the points plotted, the pattern of the points above and below this line is very similar for each crystal. In each graph, the points representing (031), (051) and (023) reflections lie below the line, the points representing (006) and (044) lie close to the line and the points representing (033) and (012) lie above the line. If Zachariasen's theory is correct, this would strongly suggest that the points are being affected by

Crystal	Gradient ($\times 10^6$)	Thickness(cm.)
1	0.062	0.046
2	0.040	0.040
3	0.068	0.023
4	0.065	0.022
5	0.050	0.0197
6	0.050	0.0192

Table 3

Crystal	Possible variation of individual gradients ($\times 10^6$)	Absolute deviation from the mean gradient ($\times 10^6$)
1	0.0123	0.0060
2	0.0051	0.0160
3	0.0125	0.0120
4	0.0112	0.090
5	0.0105	0.060
6	0.0079	0.060

Table 4

systematic errors, almost certainly in the calculated structure factor values, which were used to calculate the Q and y values. Obviously, another alternative is that Zachariasen's theory may not describe extinction properly and the distribution of the points may be a curve, instead of a straight line passing through the origin or each reflection is affected by a large angle dependent factor.

Due to these systematic errors, it was thought that a least-squares solution for the best straight line might not be appropriate and therefore the best straight line, passing through the origin, was drawn about which the points seemed to be best distributed.

If the mosaic character of the crystals was identical and if only secondary extinction was taking place, then gradients of the graphs should be the same. The gradients of the graphs were measured and are shown in Table (3).

The average gradient and standard deviation were calculated and found to be

$$\langle m_s \rangle = 0.056 \times 10^6$$
$$\sigma_s = 0.0043 \times 10^6$$

An estimate of the possible variations of the gradients of each individual graph and the absolute deviation of each gradient from the mean are shown in Table (4). The possible variations in the individual gradients are of the same order or greater than the absolute deviations from the mean. The only exception was crystal 2. This suggests that deviations from the mean gradient may be mainly because of the systematic errors in the calculated structure factors but not because of different mosaic characters. This may not be true in the case of crystal 2 which has a gradient considerably lower than the others.

Excluding crystal 2, the average value of the gradients and standard deviation were found to be 0.059×10^6 and 0.0038×10^6 respectively, which does not differ much from the values calculated including crystal 2.

Since the crystals were grown in the same way, it was thought reasonable to assume all of the crystals have the same mosaic character, and it was decided to use the average value of the gradients $\langle m_s \rangle = (0.0560 \mp 0.0043) \times 10^6$ in the calculation of extinction parameters.

Assuming the crystals are of type I, from eq. (34)

$$\langle m_s \rangle = 2g$$

$$g = 2.8 \times 10^4$$

Assuming that crystals are of type II, from eq. (35)

$$\langle m_s \rangle = (2 r_s / \lambda)$$

$$r_s = 4.3 \times 10^{-4} \text{ cm.}$$

b) Assuming only primary extinction:

The values of $(1/y^2)$ were plotted against Q for each crystal. These are shown in fig. (13). Again there were significant departures from linearity, but the pattern of the points were very similar in each graph, the points corresponding (023), (051) and (031) being below any possible best fitted line passing through the origin. Once more, Zachariasen's theory was assumed to be correct and these deviations were regarded as the systematic errors in the calculated structure factors as in the secondary extinction case.

Therefore the least-squares fitted lines were not used and the lines passing through the origin and best fitting the data were drawn about which the points seemed to be best distributed. The gradients of the graph were measured.

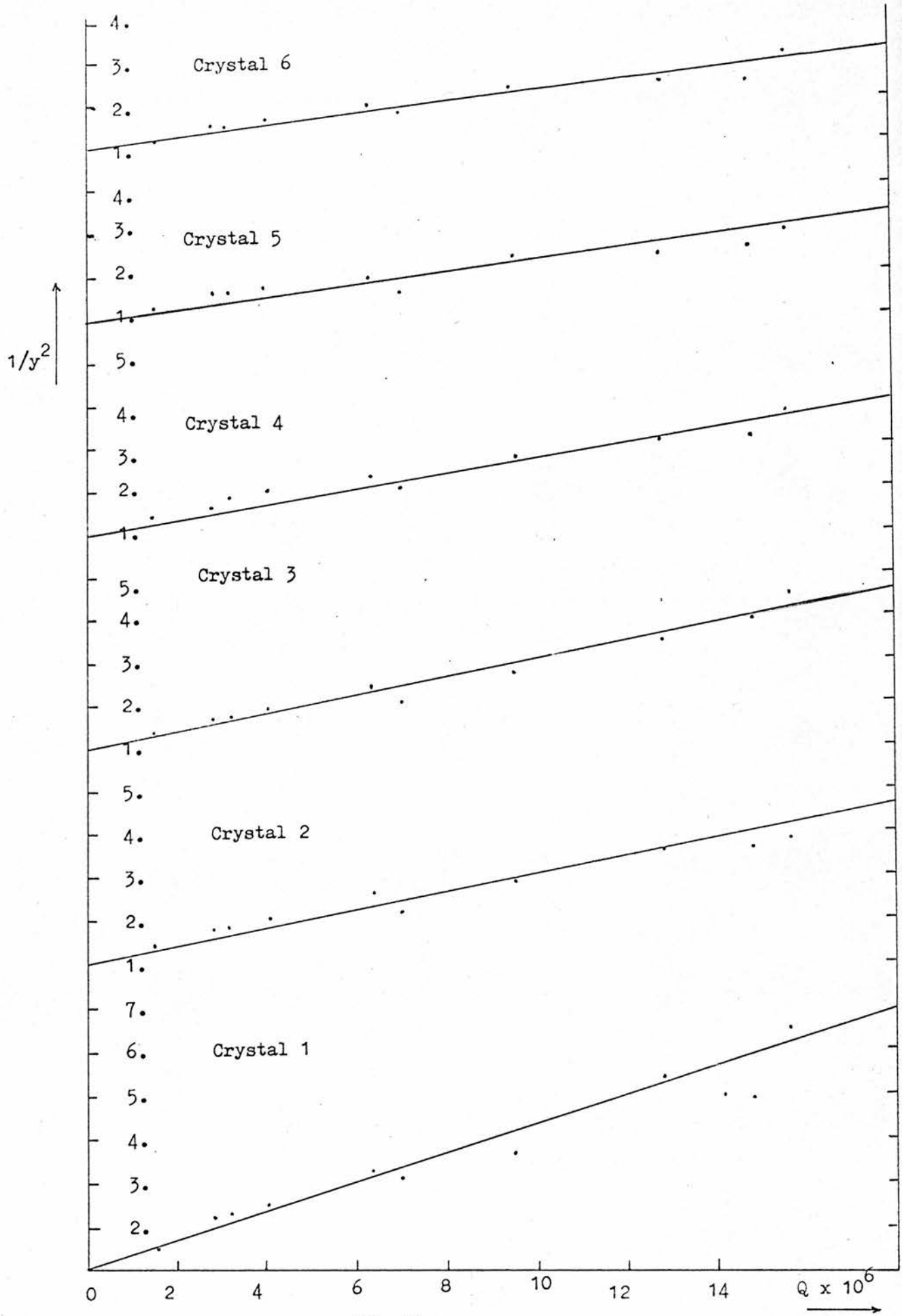

Fig.13

Graphs of y^{-2} against Q for Cu radiation

Crystal	Gradient (x 10^4)	Thickness (cm.)
1	0.328	0.046
2	0.206	0.040
3	0.202	0.023
4	0.187	0.022
5	0.134	0.0197
6	0.126	0.0192

Table 5

h k l	Condition for r	Condition for g
0 0 4	$r < 3.63 \times 10^{-4}$ cm.	$g \ll 2.36 \times 10^4$
0 3 1	$r < 3.73 \times 10^{-4}$ cm.	$g \ll 2.42 \times 10^4$
0 1 3	$r < 4 \times 10^{-4}$ cm.	$g \ll 2.6 \times 10^4$
0 5 1	$r < 4.63 \times 10^{-4}$ cm.	$g \ll 3 \times 10^4$
0 2 3	$r < 5.4 \times 10^{-4}$ cm.	$g \ll 3.5 \times 10^4$

Table 6

They are shown in Table (5). Average gradient $\langle m_p \rangle$ and standard deviation σ_p were calculated and found to be

$$\langle m_p \rangle = 0.197 \times 10^4$$

and

$$\sigma_p = 0.027 \times 10^4$$

from eq. (36)

$$\langle m_p \rangle = 3\, r^2/\lambda$$

$$r_p = (3.2 \pm 0.5) \times 10^{-3} \text{cm}.$$

The standard deviation in the average gradient assuming secondary extinction was 7.5% while, for primary extinction, the standard deviation in the average gradient was 13.7% and this clearly shows that the assumption that only secondary extinction is present yields more consistent results. Also, inspection of Table (5) shows that the gradients are thickness dependent. Thickness dependence of the gradients in Table (5) is almost linear, the only exception being the gradient of crystal 2 again, which does not fit the pattern, having a considerably small gradient for its thickness.

As stated before, the integrated intensities of the strong reflections were measured to an accuracy of two percent. Therefore the limiting measurable value of y can be obtained from

$$\Delta F^2/F_c^2 = \left[(F_c^2 - F_{ob}^2)/ F_c^2\right] = 1 - y = 0.02$$

from this

$$1 - 1/\sqrt{1 + 2x} = 0.02$$

$$x = 0.02$$

This means that two percent accuracy restricts the value of x such that $x < 0.02$ in order to be able to neglect primary extinction. From this, for negligible primary extinction the limits of r, and, using these limits and definition

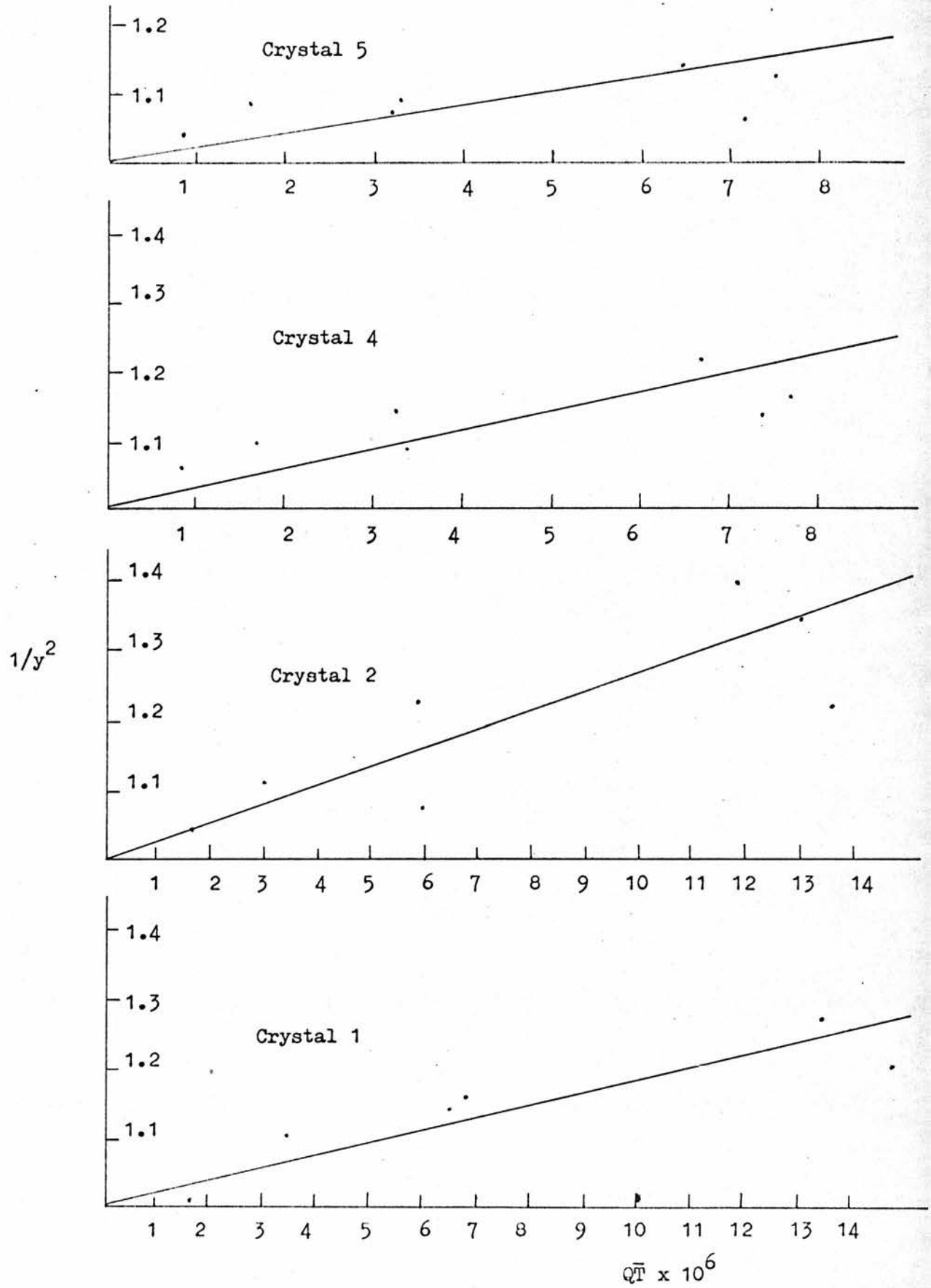

Fig. 14 a

Graphs of y^{-2} against QT for Mo radiation

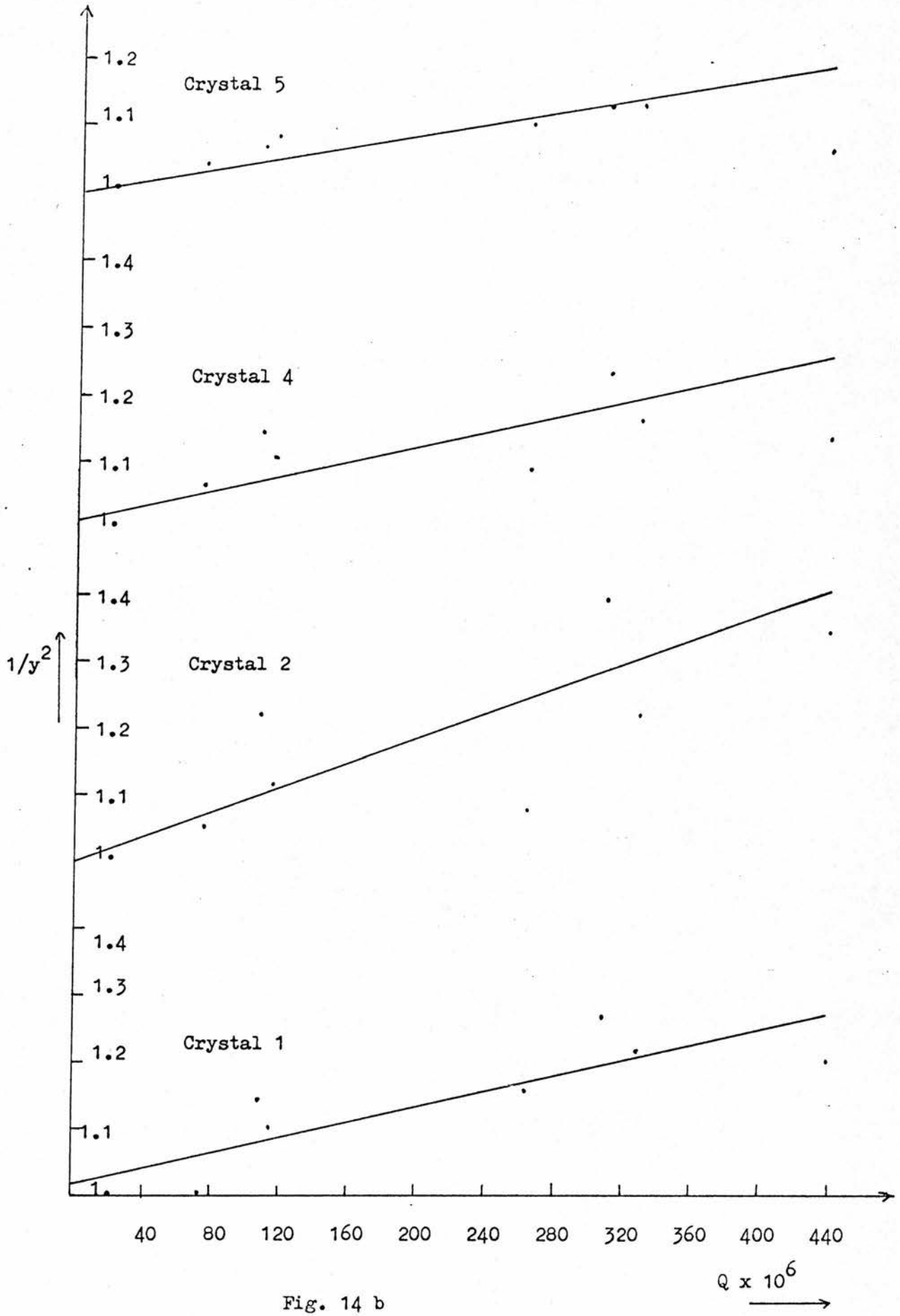

Fig. 14 b

Graphs of y^{-2} against Q for Mo radiation

h k l	$Qx10^6$ cm.	crystal 1		crystal 2		crystal 4		crystal 5	
		$1/y^2$	$Q\bar{T}$	$1/y^2$	$Q\bar{T}$	$1/y^2$	$Q\bar{T}$	$1/y^2$	$Q\bar{T}$
0 3 1	331.13	1.216	15.44	1.214	13.6	1.158	7.7	1.120	7.5
0 0 4	438.96	1.199	14.8	1.339	13.0	1.131	7.4	1.057	7.2
0 1 3	310.13	1.269	13.4	1.390	11.8	1.223	6.7	1.133	6.5
0 5 1	266.3	1.162	6.8	1.070	6.0	1.089	3.4	1.088	3.3
0 1 2	108.3	1.139	6.7	1.225	5.9	1.137	3.3	1.072	3.2
0 2 4	114.57	1.104	3.4	1.116	3.0	1.100	1.7	1.080	1.6
0 4 4	76.83	1.005	1.8	1.054	1.6	1.066	0.9	1.037	0.88

Table 7

Assuming secondary extinction		Assuming primary extinction	
Crystal	Gradient($x10^4$)	Crystal	Gradient
1	2.	1	375
2	2.75	2	541
4	2.62	4	875
5	1.75	5	541
Average gradient $\langle m_s \rangle_{mo}$ $=2.28x10^4$ Standard deviation $(\sigma_s)_{mo}$ $=0.242 \times 10^4$ Assuming type I $(g)_{mo} = 1.14 \times 10^4$ Assuming type II $(r_s)_{mo} = 0.81 \times 10^{-4}$ cm.		Average gradient $\langle m_p \rangle_{mo}$ $=583$ Standard deviation $(\sigma_p)_{mo}$ $=105$ $(r_p)_{mo} = 1.17 \times 10^{-3}$ cm.	

Table 8

of type I crystal ($r/\lambda g \gg 1$), the limits of g were calculated for strong reflections. Results are shown in table (6).

Comparison of the values in table (6) with the values obtained assuming secondary extinction only, either type I or type II, shows that at least for strong reflections primary extinction is not negligible if Zachariasen's parameter have physical meaning.

MoKα data:

The most extinguished seven reflections, their ($1/y^2$), Q and $Q\bar{T}$ values are shown in Table (7). As in CuKα data, the values of $1/y^2$ were plotted against $Q\bar{T}$ assuming only secondary extinction is taking part and were plotted against Q assuming only primary extinction is taking part, fig. (14). Again assuming Zachariasen's theory is correct, the departures from linearity were regarded as the systematic errors in the calculated structure factors and the best fitted lines were drawn as in CuKα data. The results from these graphs are shown in Table (8). The standard deviations $(\sigma s)_{mo}$ and $(\sigma p)_{mo}$ lead to 10.6% and 18% errors in the mean respectively, implying the lines drawn assuming secondary extinction only fit the data better.

If the crystals are of type I or type II, the values obtained should be consistent for both Cu and Mo radiations. Comparison of the results in table (8) with the results in tables (3) and (5) shows that this is not the case, possibly suggesting the material is of an intermediate type. Therefore, using $(r_s)_{cu}$ and $(r_s)_{mo}$ as r_1^* and r_2^* in eq. (33) respectively, the parameters $r_{int.}$ and $g_{int.}$ were calculated assuming the material is of intermediate type

$$r_{int.} = (1.7 \pm 0.3) \times 10^{-4} \text{ cm.}$$

$$g_{int.} = (1.03 \pm 0.15) \times 10^{4}$$

However, the discrepancies in the g values are less than those for the r values suggesting that the crystal may tend more towards type I than type II.

It can therefore be concluded that the extinction in the data sets is probably predominantly secondary since a path length dependence has been detected. By studying the extinction at two wavelengths, it has been shown that the crystal is neither a type I nor a type II crystal but conforms to an intermediate type and therefore values of block size and of mosaic spread have both been estimated.

This mosaic block size, determined assuming only secondary extinction, is too large to permit this assumption and it must be concluded that some primary extinction must be present.

These conclusions are based on the premise that Zachariasen's equations are correct and a possible indication as to the reliability of these equations may be obtained from a comparison of the parameter obtained from the analysis with these from experimental observations.

As stated before, the mosaic crystal model is the common way in extinction studies to describe the geometrical array of imperfections which leads to incoherence of the waves from different regions of the crystal since the detailed information on the imperfection structures of the materials is not available. Although the idea of mosaic blocks is unrealistic, an estimate of the size of the blocks should in some way provide a consistent measure of the density of imperfections in the crystal.

In some of the work on extinction, the r* parameters obtained following Zachariasen's procedure had been found to be physically unreasonable (Lawrence, Killean and Sharma (1972), Becker and Coppens (1974))

Zachariasen's theory cannot be regarded as a realistic theory if it does not lead to physically reasonable parameters which will be consistent with the real imperfection structure of the material. In most of the work on the subject, these parameters were obtained from least squares refinement. Obviously, these least squares analysis in which extinction parameters are included can have very little validity unless Zachariasen's theory give physically reasonable r* values, although this procedure may improve the fit between the observed and calculated structure factors.

It was decided to check whether the parameters obtained using Zachariasen's theory agree with the physically observed values or not. It was thought that the parameter r can be obtained from the dislocation densities of the material assuming a one to one correspondence between the mosaic domain size and the dislocation density, while the parameter g can be obtained from the measurements of the mosaic spread of the crystal.

Dislocations in the materials can be observed directly by means of X-ray transmission topography, Lang (1957). Dislocations induce strains around the core of the dislocation line which is a very highly distorted region of the crystal. This core may have a diameter of a few angstroms and since it is very highly distorted, does not contribute the diffraction phenemena, but the strains induced are important a few microns from the core, giving

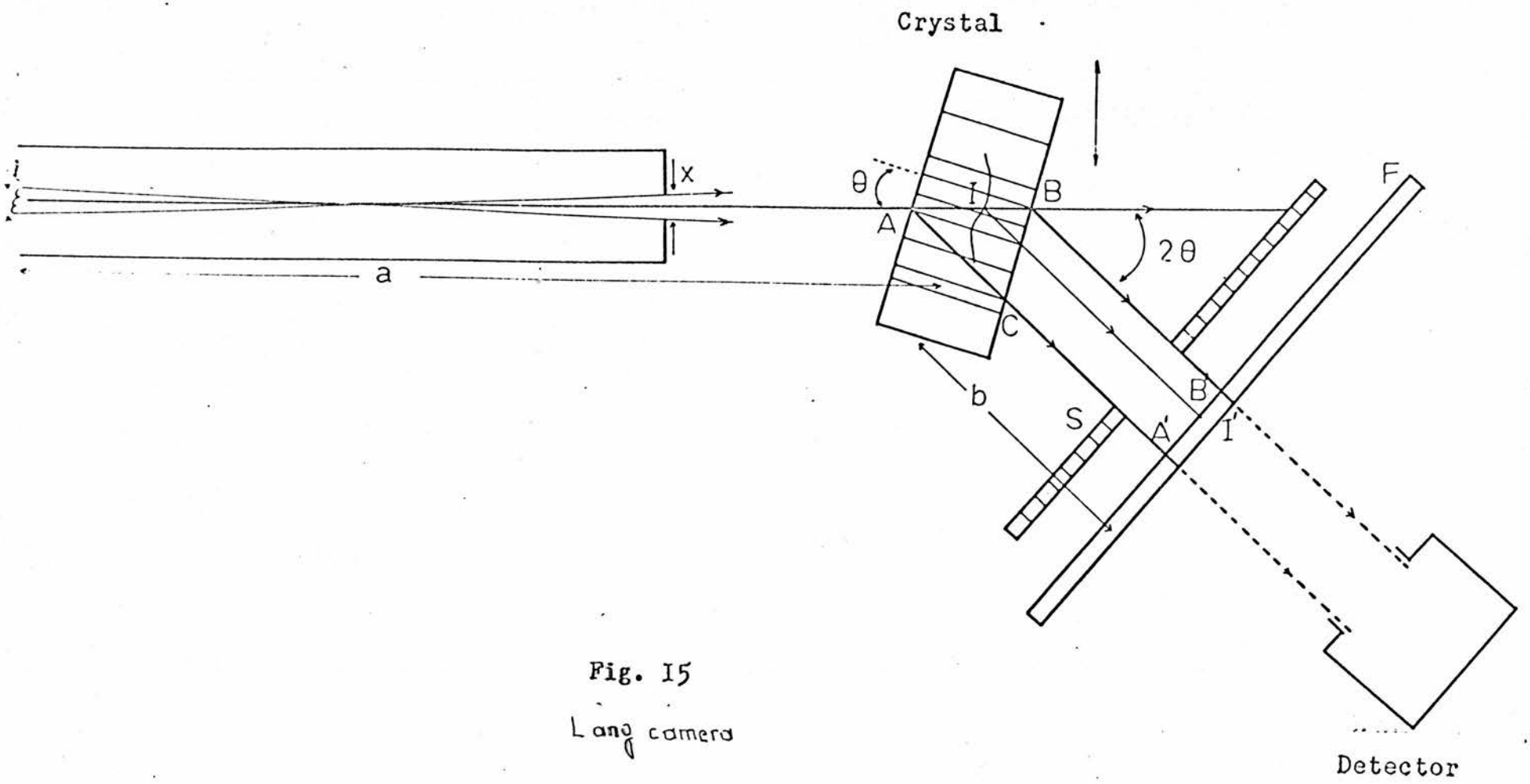

Fig. 15

Lang camera

rise to a distorted region around the core to bring about important perturbations in the diffraction of X-rays by the perfect crystal.

These deformed regions around the dislocation lines give rise to the images of dislocations, diffracting the X-rays kinematically. The perfect regions of the crystal will diffract the X-rays dynamically, therefore the integrated intensities from thekinematically diffracting regions of the crystal will be higher than the integrated intensities from perfect regions because of extinction effects and will form the direct images of dislocations when they are recorded on a photographic plate, because of these "extinction contrasts".

Further, it is possible to distinguish the regions which are misoriented with respect to each other from their "orientation contrasts" on the topographs. In a region containing local misorientations, the integrated intensity will vary from point to point depending upon the deviation from the ideal Bragg angle at the point.

The topographic method of recording the imperfection contents of the material, using well collimated characteristic radiation and Laue type reflections only is called transmission topography which was improved by Lang (1959). The apparatus used is called Lang Camera, Fig (15). It has a circular base which is marked in degrees. The height of this base can be adjusted by means of three levelling screws. The platform carrying the goniometer head on which the specimen crystal is mounted, is at the centre of this circular base. A detector arm is mounted concentrically which can move to a given 2θ value around

this circular base, carrying a detector to detect the peak maxima of the diffracted beam. The crystal orientation is so arranged that the diffracted beam is received in this horizontal plane.

The main diffraction geometry is simple. A narrow beam of characteristic radiation, coming from the X-ray source which is a fine-focus X-ray tube having focal spot dimensions of 0.3 x 0.8 mm, is obtained by means of a long collimator having a narrow slit at its end. This narrow beam cuts through the crystal along the path AB. The crystal setting on the platform is such that this ray is Bragg-reflected by diffracting planes which are normal to the X-ray entrance and exit surfaces. Then, the diffracted ribbon of X-rays passes through the slits where the main beam is stopped, and is recorded as a strip of blackening of width A'B' on the photgraphic plate giving rise to the image of any dislocation in the triangle ABC, the direct image coming from the intersection point I of the main beam and the dislocation dynamic images which accompany the direct images as a shadow come from the intersection points of wave-fields and dislocation in the triangle ABC. If the specimen crystal is a plate of thickness t, width of the topograph A'B' is simply given by

$$A'B' = 2t\sin\theta$$

This type of topography in which the crystal and the photographic plate are kept stationary is called a "section topograph". In the case of section topographs only a very narrow portion of the crystal diffracts X-rays, so the images of imperfections can be obtained only for this narrow region. In order to scan a larger area of the

specimen crystal, the crystal and the photographic plate are driven back and forth across the X-ray beam while the slit S stays stationary. This motion is achieved by pushing forward the platform which carries the crystal, by a micrometer screw head driven by a d.c. motor against a spring. The range of the scan can be adjusted by the limit switches which reverse the motion of the platform at a certain point. When the micrometer head moves back the platform is pushed back by the spring, thus the crystal is moved back and forth across the X-ray beam between two limits many times and the diffraction topograph from a large volume of the crystal so obtained is called a "projection topograph". In section topographs a dislocation is revealed only by the direct image I' coming from the point I where the ribbon of X-rays AB, cuts the dislocation, as a relatively intense black spot while in the projection topographs, the full length of the dislocation can be seen. Thus the projection topograph is a super imposition of many successive section topographs. The complete outline of features of mosaic domains can be seen either by their orientation or extinction contrasts in the projection topographs.

The width of the slit S can be arranged so that some certain parts of the diffracted ribbon of X-rays can be stopped and therefore, elimination of the images coming from surface damage which are blackening the topographs , and the images of the imperfections lying in the depths of the crystal can be observed.

The vertical resolution, Rv, i.e. resolution in the

direction perpendicular to the plane of incident and diffracted beams is purely geometrical and is given by

$$Rv = h\ (b/a)$$

where h is the apparent height of the focal spot of the X-ray source, b is the distance from the specimen crystal to photographic plate and a is the distance from the focal spot to the crystal.

Horizontal resolution i.e. the topographic resolution in the plane of incident and diffracted beams is limited by the angular seperation of $K\alpha_1$ - $K\alpha_2$ doublet. This doublet gives rise to double images on the photographic plate each corresponding to $K\alpha_1$ and $K\alpha_2$ lines seperately. Generally X-ray topographs are classified as "low - resolution" if these $K\alpha_1$, $K\alpha_2$ images simultaneously appear on the topograph and "high-resolution" when such superimposition is eliminated by suppressing $K\alpha_2$ line.

Reducing the horizontal divergence of the X-rays, $K\alpha_2$ line can be suppressed. The angular seperation of the doublet can be obtained as

$$\Delta\theta = \Delta\lambda / 2\ d\ \mathrm{Cos}\theta$$

where $\Delta\lambda$ is the wavelength difference between $K\alpha_1$ and $K\alpha_2$ lines. Therefore, the horizontal divergence of the main beam should be smaller than this angular seperation in order to suppress $K\alpha_2$ line. Horizontal divergence of the main beam is given by

$$\Psi_H = (\ell + x) / a$$

where ℓ is the width of the focal spot of the X-ray source x is the width of the collimator slit and a is the distance between the focal spot and the specimen crystal.

When the $K\alpha_2$ line is eliminated, the horizontal resolution is determined by the wave length spread. If $d\lambda$ is the wavelength range corresponding to the full width at half maximum intensity of the X-ray emission line profile, the range of the corresponding Bragg angles $d\theta$ is given by

$$d\theta = \mathrm{Tan}\theta \left(d\lambda / \lambda \right)$$

This corresponds to the image of a point on the crystal being spread horizontally into a length of

$$ds = b\, d\theta$$

By setting the photographic plate as near as possible to the crystal and choosing the reflections having small Bragg angles this resolution can be of the order of a few micrometers.

On the photographic plates, thick nuclear emulsions can absorp a large portion of the X-rays, so most of the diffracted rays can be recorded efficiently, also, thick nuclear emulsions are preferable to thin emulsions from the statistical limitations point of view. Although they need long developing and washing times, thick nuclear emulsions are usually used in X-ray topography.

From the topographs, one gets the projection of the imperfection contents of the crystal in two dimensions. By taking stereo pairs of projection topographs, (Lang (1959), Haruta (1965)) three - dimensional information can be obtained.

In the present experiments, the distance a from the focal spot to the specimen was 70 cm. Focal spot width was 0.4 mm and the width of the collimator slit was 0.2 mm. With these conditions, the $K\alpha_2$ component of the radiation

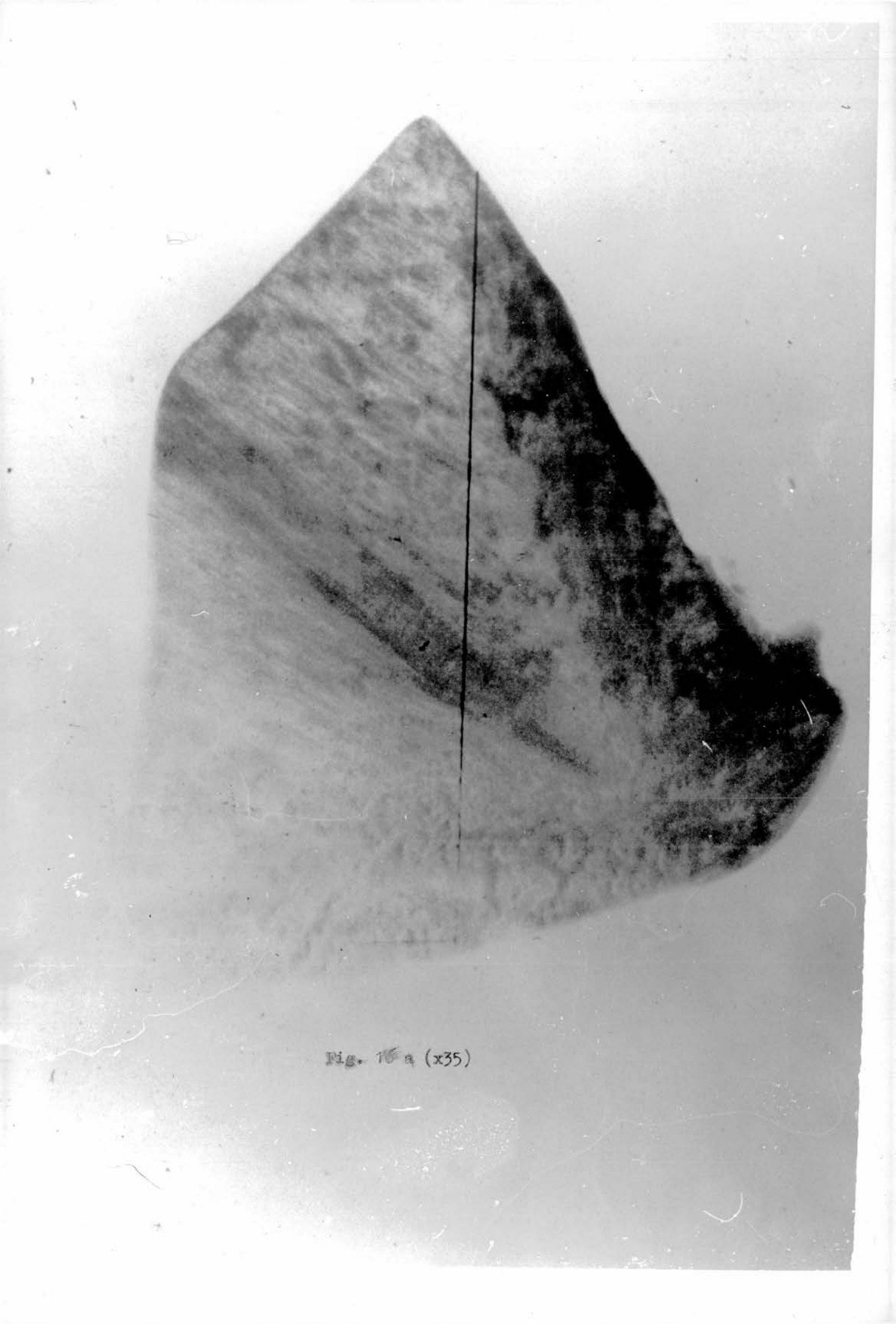

Fig. 16 a (x35)

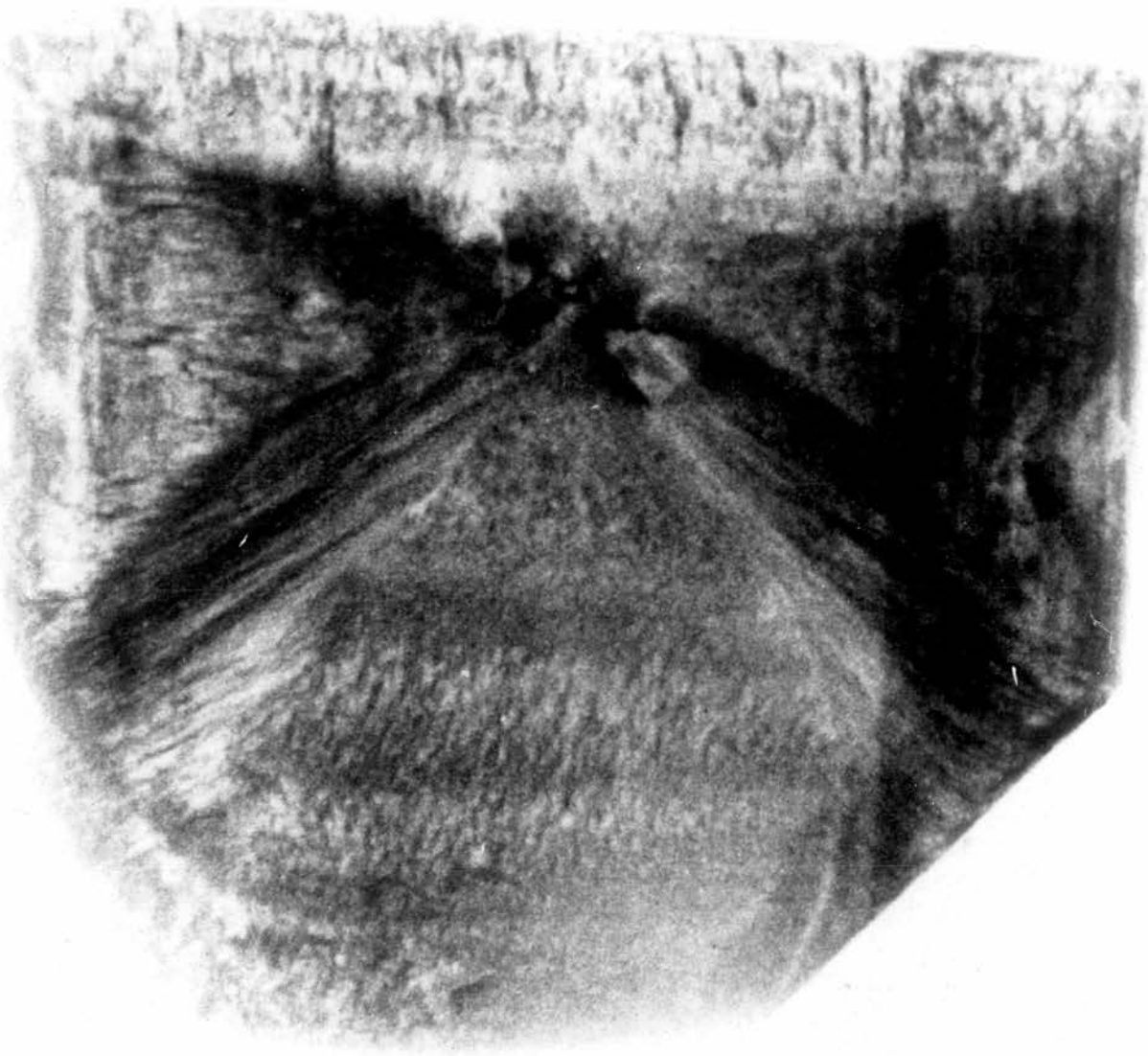

Fig.16 b (x30)

could not be eliminated for the (002) reflection used. The distance a was the maximum distance since for larger distances the diffracted intensity was very weak. The photographic plates used were thick Ilford L 4 nuclear plates. Topographs for (002) reflection are shown in Fig (16). Although there is a lot of blackening on the topographs due to the surface of the crystals, dislocations can clearly be observed in all of the topographs. Most of the observed dislocations start from a point and lie parallel to the faces of the crystal.

The direct observation of dislocations with this method suggests that the dislocation density can not be larger than 10^6 cm^{-2} since in larger dislocation density, topograph will be completely black. The lines observed were counted under a microscope and at various points of various topographs, these average dislocation densities were found

$$2.3 \times 10^5 \ cm^{-2}$$
$$3.0 \times 10^5 \ cm^{-2}$$
$$1.3 \times 10^5 \ cm^{-2}$$
$$3.6 \times 10^5 \ cm^{-2}$$
$$5.0 \times 10^5 \ cm^{-2}$$

$$\text{average} = 3.0 \times 10^5 \ cm^{-2}$$

It should be noted that these are maximum values, since the topograph is a projection of a volume on the photographic plate. The above values are the square of the number of dislocations per cm. If we assume an approximate relationship between the dislocation density, D, and the block size, r, is

$$D \cong 1/\pi r^2 \ ,$$

then the average block size in the crystal will be of

10.3×10^{-4} cm. This can be compared with the values of r from Zachariasen's equations.

This value can be seen to be between the values for Cu radiation -

$$(r_s)_{cu} = 4.3 \times 10^{-4} \text{ cm.}$$

and $$(r_p)_{cu} = 3.18 \times 10^{-3} \text{ cm.}$$

For the Mo radiation, the value of r obtained assuming type II secondary extinction is more than an order of magnitude smaller than the experimental value. Blocks of this size would be so small that no contrast would have been visible on the topograph and it must be concluded that the crystal cannot be of type II (For the Cu data, the dislocation density corresponding to the block size from Zachariasen's equation is also too small to be measured topographically) This conclusion is supported by the better agreement between the g values for the two radiation than between the r values.

The block sizes determined assuming primary extinction for both radiations,

$$(r_p)_{cu} = (3.2 \pm 0.5) \times 10^{-3} \text{ cm.}$$

and $$(r_p)_{mo} = (1.2 \pm 0.2) \times 10^{-3} \text{ cm.}$$

are large enough to be measurable topographically and the value for the Mo radiation agrees very well with the experimental value. The discrepancies between the two values could be due to errors in the angle dependence of extinction in Zachariasen's theory, these errors being more important for the Cu radiation since, for this radiation, the scattering angles are greater.

Measurement of diffraction profiles

In principle, the measurement of the diffraction

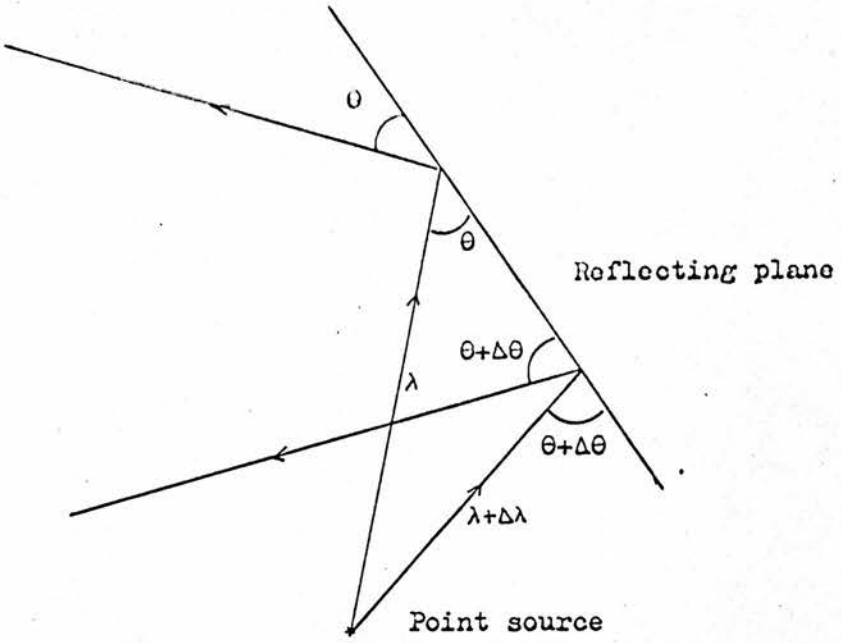

Fig.17

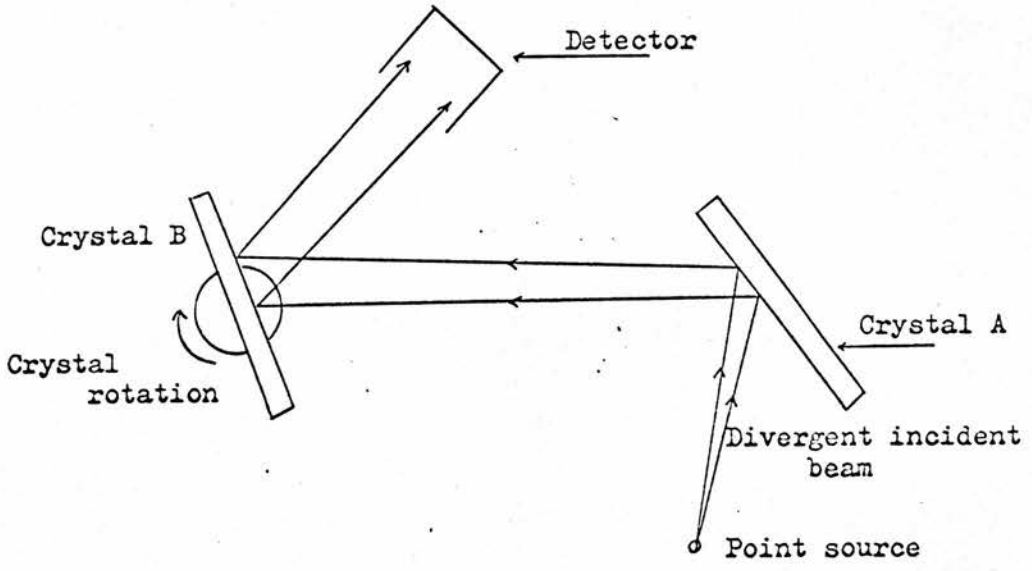

Fig. 18

Ray diagram showing dispersion

and schematic diagram of two crystal

spectrometer

profile of a crystal is simple. If the crystal is placed in the path of a monochromatic, parallel beam of X-rays and set at the correct Bragg angle and slowly rotated through this position, the reflection will occur over a range of crystal settings about the exact Bragg angle giving the diffraction profile. The mosaic spread of the crystal can be obtained from the width of this diffraction peak at intensities which are half the maximum intensity.

The difficulties in the measurments of this kind are -

1. The divergence of the beam from the source.

If the incident radiation is divergent, various mosaic blocks of the crystal having different alignments will diffract the beams falling upon them at the correct Bragg angle, at every setting of the crystal. Obviously, in order to be able to measure mosaic spread, strictly parallel incident radiation is required.

2. Finite width of the incident radiation:

Although, one can cope with the divergence of the incident radiation, e.g. using a strong reflection from a perfect crystal as the incident beam, it is not practically possible to obtain a strictly parallel and monochromatic X-ray beam because of dispersion due to lack of homogeneity of the beam from the source. A beam of wave length λ which is falling on the perfect crystal at a glancing angle θ and a beam of wave length $\lambda+\Delta\lambda$ with a glancing angle $\theta+\Delta\theta$ will satisfy Bragg law and will be diffracted by the same diffracting planes of the perfect crystal, fig (17). The resulting divergence of the diffracted beam because of the natural width of the wavelength used can be calculated from Bragg's law:

$$2\,d\,\sin\theta = n\lambda$$

$$2\,d\,\cos\theta\,d\theta = n\,d\lambda$$

$$\therefore\ d\theta = (d\lambda/\lambda)\tan\theta$$

For example, even from a perfect crystal, for a scattering angle of about 15° and copper radiation

$$\left(\frac{d\lambda}{\lambda}\right) \doteqdot 4 \times 10^{-4}$$

$$d\theta \doteqdot 20'' \text{ of arc.}$$

These difficulties have been largely overcome by the construction of a two crystal spectrometer.

Two crystal spectrometer:

The main geometry is shown in fig (18). Crystal A is a perfect crystal. Divergent radiation from a point focus falls upon this crystal and is diffracted as a ribbon of X-rays which has a small divergence in horizontal direction due to the finite width of the wavelength used. Vertical divergence is not important since the measurments are carried out in the equatorial plane only. Specimen crystal, B, is placed in the path of this diffracted beam at the diffracting position and can be rotated by means of a stepping motor, in steps of 3" of arc about this diffracting position. The diffraction profile from crystal B can then be measured by a scintillation counter in the horizontal plane.

In the present experiments, CuKα radiation from a point focus used. Crystal A was a perfect silicon crystal reflecting in (111) position and having zero dislocation density as quoted by the manufacturers. Crystal B was the D(+) tartaric acid crystal. There are two possible different ways of setting specimen crystal B. In one, illustration by fig (19), the incident ray PO_1 and the

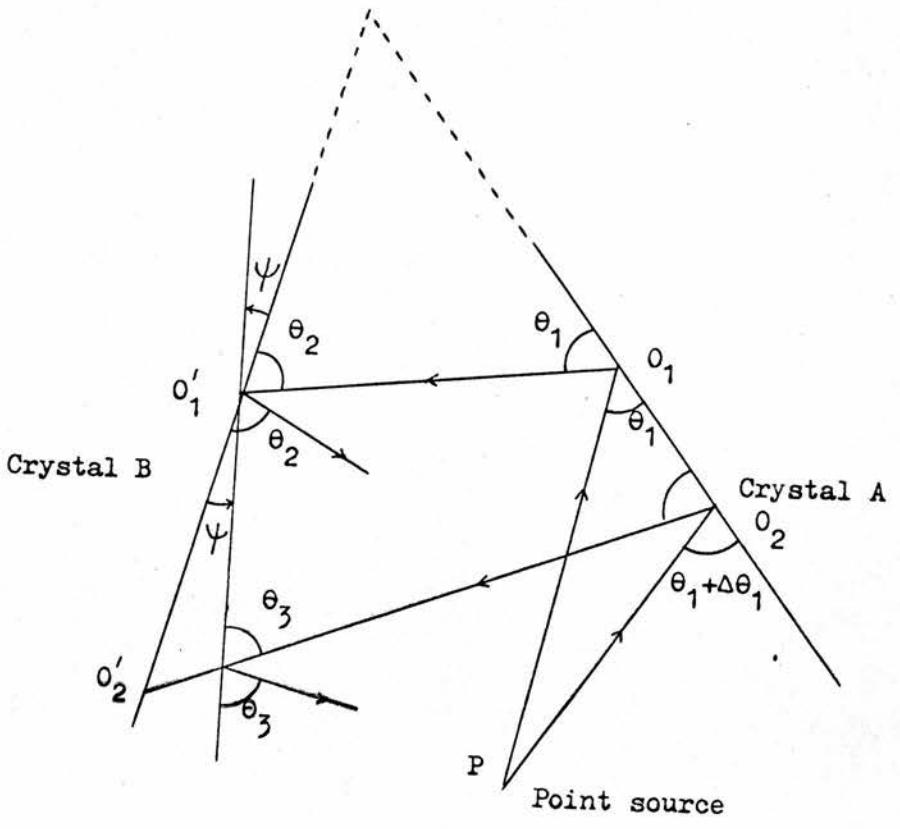

Fig. 19

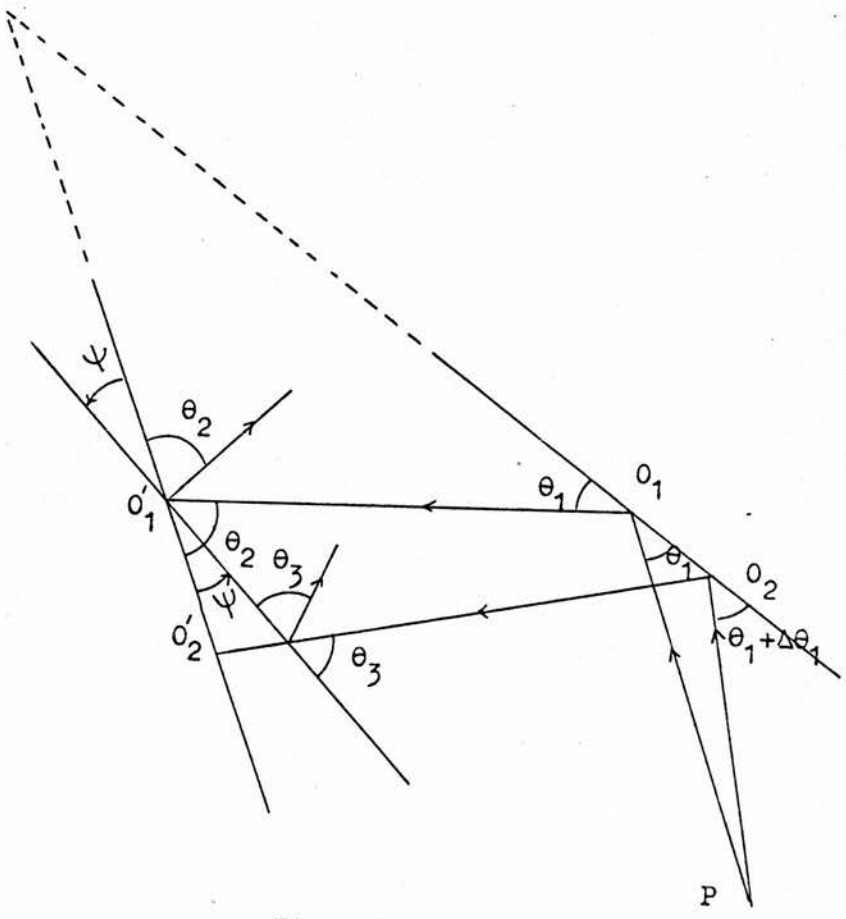

Fig. 20
Ray diagrams of (m,n) and (m,-n) settings

reflected ray from crystal B, lie on the same side of the ray O_1O_1' passing between two crystals while in the second case which is illustrated by fig (20) they lie on opposite sides of O_1O_1' . These two types of settings are referred to as (m, n) setting and (m, -n) setting respectively.

In fig (19) O_1O_1' represents a beam of wavelength λ, diffracted by crystal A with a Bragg angle of θ_1. This beam is diffracted by crystal B with a Bragg angle of θ_2. Since the incident radiation upon crystal A is divergent, a beam of wavelength $(\lambda+\Delta\lambda)$, will also be diffracted if it falls on crystal A at an angle of $(\theta_1+\Delta\theta_1)$. O_2O_2' represents such a beam. If we calculate the rotation Ψ which is required for O_2O_2' to be diffracted by crystal B, with a Bragg angle θ_3

$$\Psi = \theta_3 - \theta_2 + \Delta\theta_1 = \Delta\theta_2 + \Delta\theta_1$$

which shows that dispersion is more than the single reflection case in (m,n) setting.

In fig (20), rotation Ψ required for the beam O_2O_2' to be reflected can be found as:

$$\Psi = \theta_3 - \theta_2 - \Delta\theta_1 = \Delta\theta_2 - \Delta\theta_1$$

which shows that in (m,-n) setting overall dispersion is equal to the difference of dispersions due to single reflections from each crystal.

When the reflecting planes of crystals A and B are parallel

$$\theta_2 = \theta_1$$

$$\Delta\theta_2 = \Delta\theta_1$$

$$\therefore \quad \Psi = 0$$

This is a very important property of double crystal spectrometer. Dispersion is absent in parallel setting.

Therefore, the width of the reflection curve will give a measure of mosaic spread of the specimen crystal if the first crystal is perfect.

If we assume that first crystal is not ideally perfect, but has a mosaic spread as well, assuming a Gaussian distribution of block orientation for both of the crystals, the effects on the overall reflection curve can be calculated as follows:

Let the incident radiation be given by

$$I(\lambda) = I_0(\lambda_0) \exp[-a_1(\lambda - \lambda_0)^2]$$

and the block orientation distribution given by

$$N(\theta) = N(\theta_0) \exp[-a_2(\theta - \theta_0)^2]$$

Since

$$d\theta = (d\lambda / \lambda) \tan\theta$$

$$\theta - \theta_0 = (\tan\theta/\lambda)(\lambda - \lambda_0)$$

therefore

$$N(\theta) = N(\theta_0) \exp[-a_2(\theta - \theta_0)^2]$$

$$I(\theta) = I(\theta_0) \exp[-a_1(\lambda^2/\tan^2\theta)(\theta - \theta_0)^2] .$$

Using a transformation

$$\phi = \theta - \theta_0 \quad ,$$

then

$$N(\phi) = N_0 \exp[-a_2\phi^2]$$

$$I(\phi) = I_0 \exp[-b\,\phi^2]$$

where

$$b = (a_1 \lambda^2)/ \tan^2\theta$$

Then, since the reflection curve is given by the convolution

$$R(\Psi) = \int_{-\infty}^{\infty} N(\phi)\, I(\Psi - \phi)\, d\phi$$

$$R(\Psi) = \text{constant x } \exp\left[-(a_2 b \Psi^2)/(a_2 + b)\right]$$

can be found. According to this result, the resultant

h k l	tanθ	w	dθ	$K\alpha_1$-$K\alpha_2$ separation	
				Obs.	Calc.
0 0 2	0.2605	24"	0"		
-1 0 2	0.2623	24"	0.15"		
0 0 3	0.4060	30"	12"	74.4"	73"
-2 0 3	0.4307	33"	14"	87"	84"
-3 0 3	0.4921	42"	19"	118"	120"
0 0 4	0.5820	54"	24"	160"	168"

Table 9

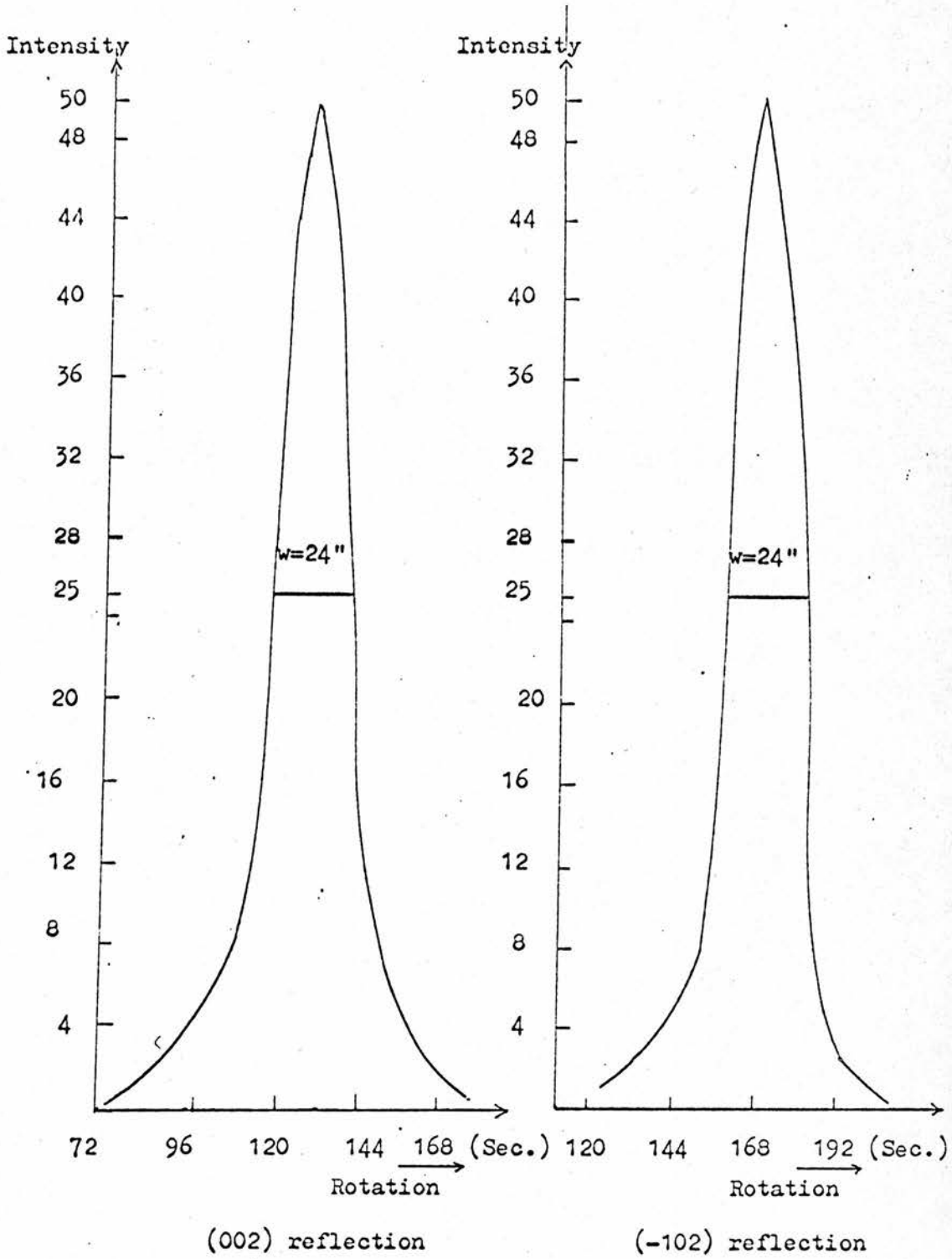

Fig. 21a

Fig. 21b

Diffraction profiles

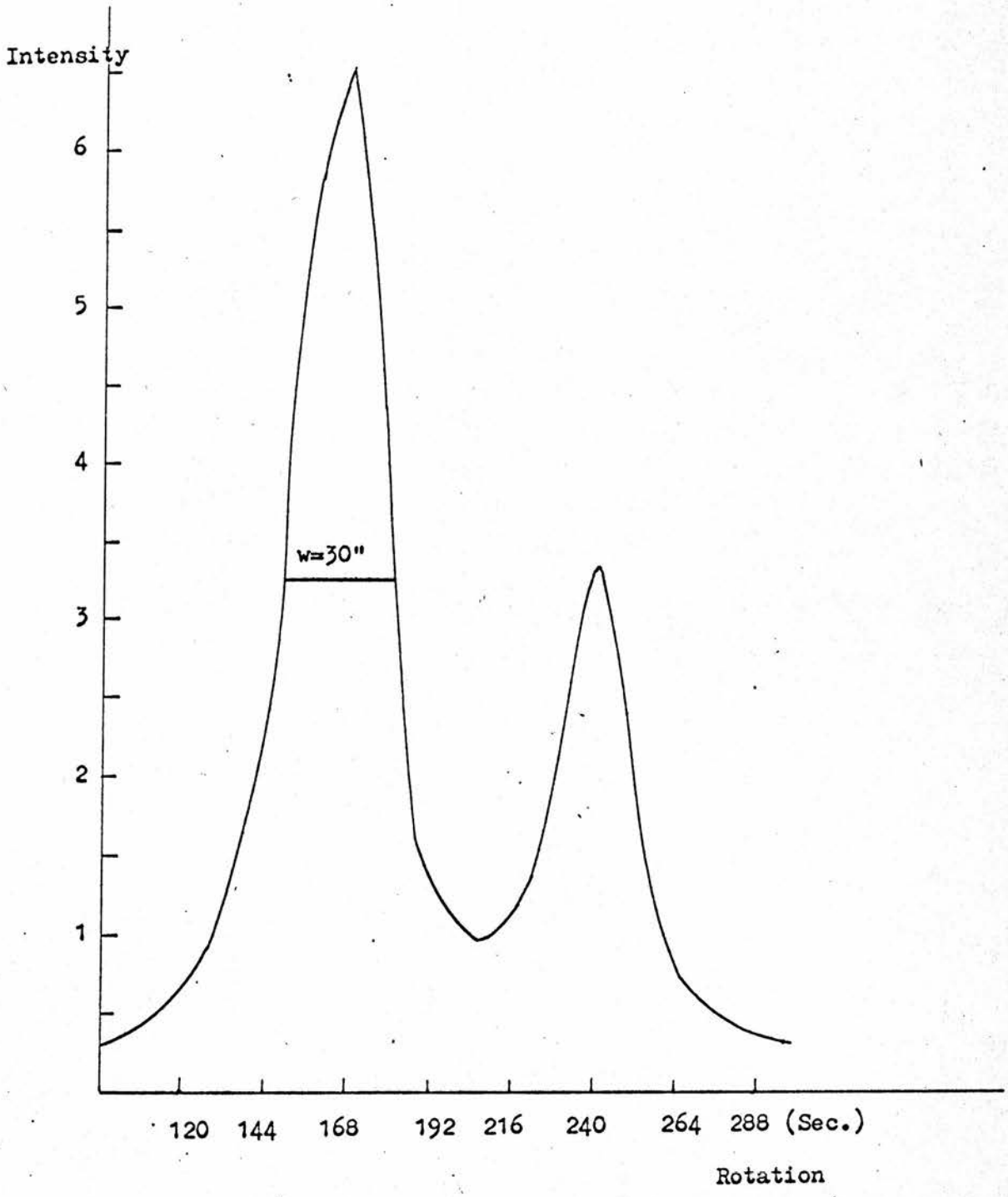

(003)reflection

Fig.21 c

Diffraction profile

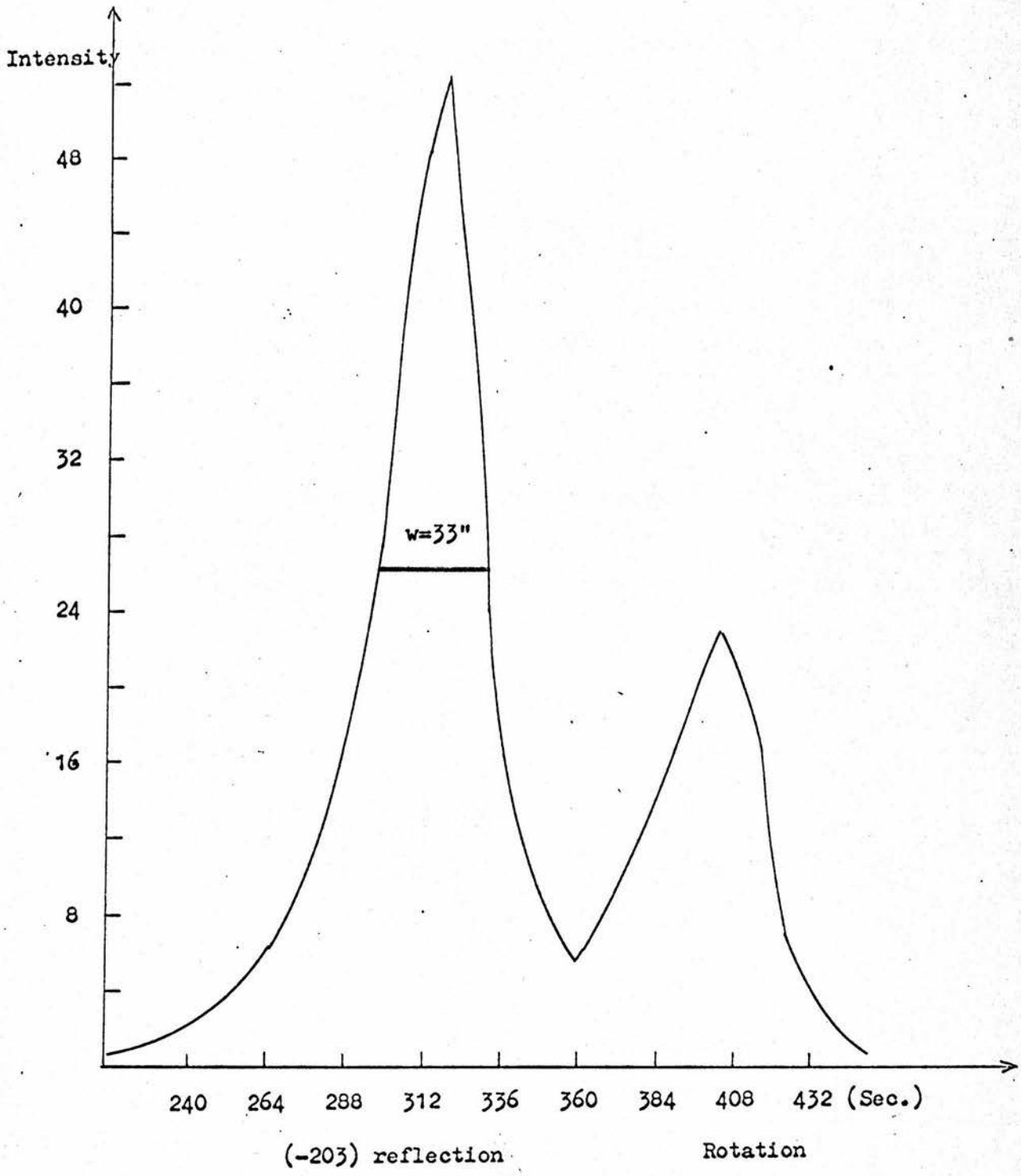

Fig. 21d

Diffraction profile

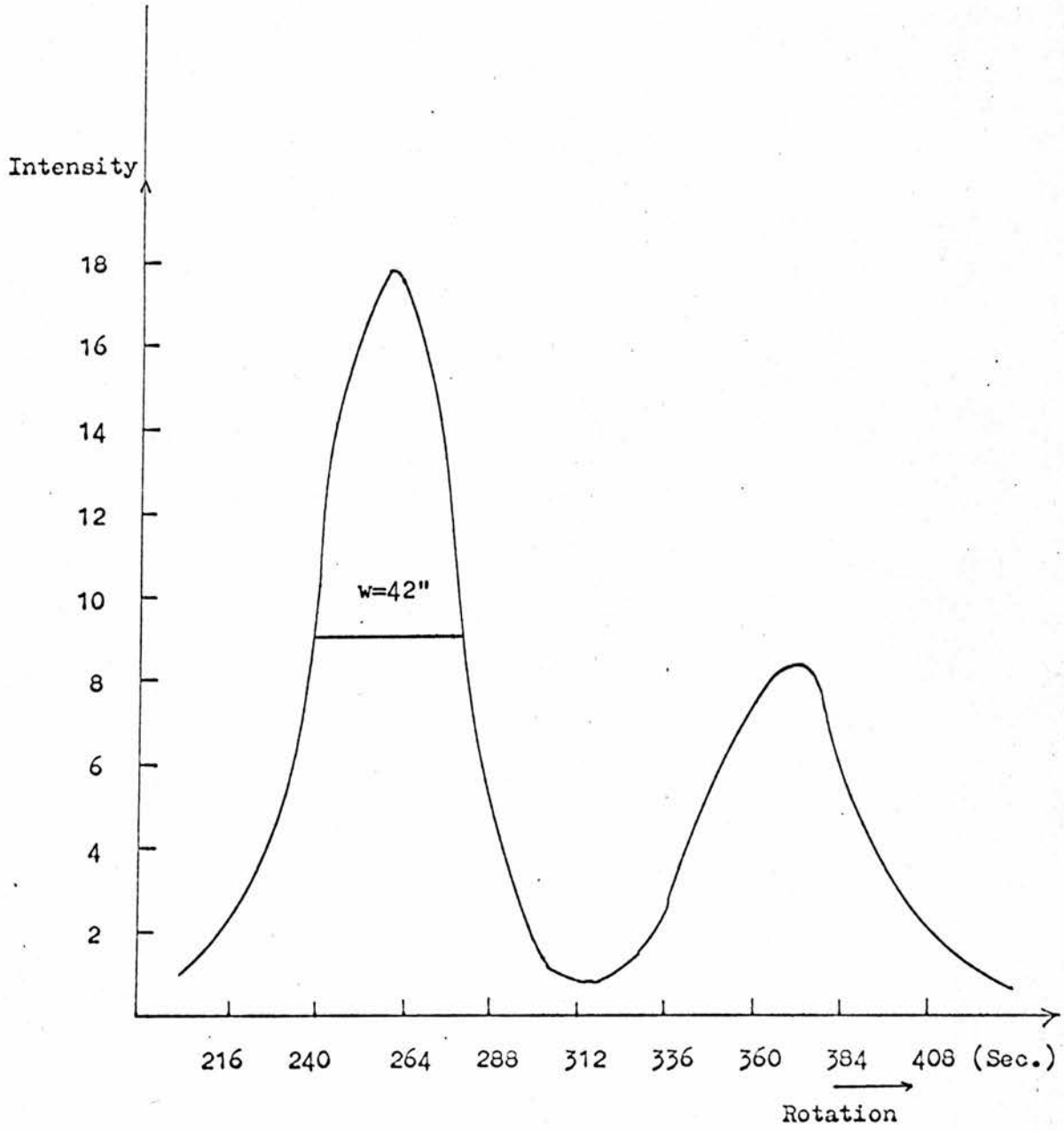

(-303) reflection

Fig. 21 e

Diffraction profile

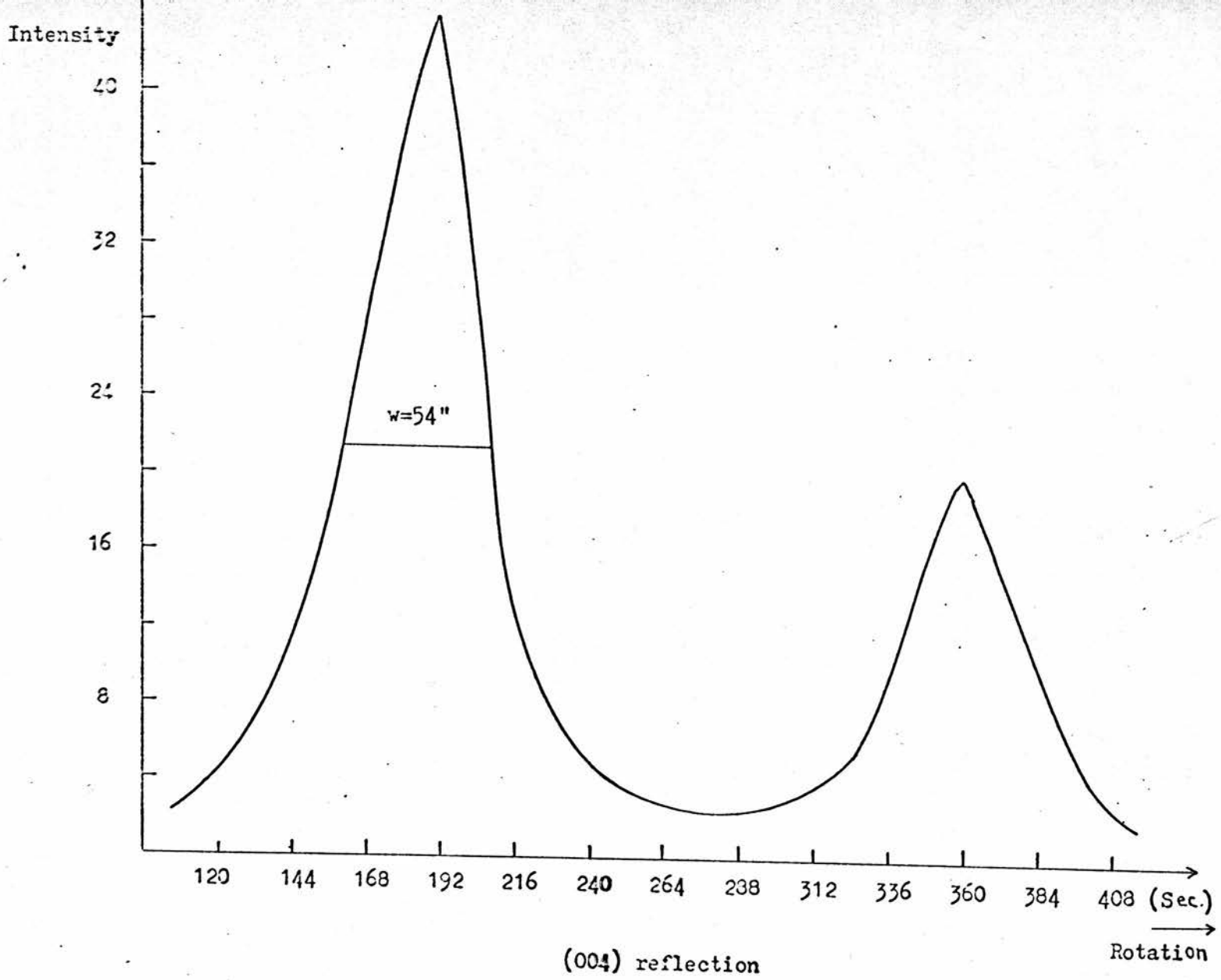

(004) reflection

Fig. 21 f

reflection curve has a parameter B which is given by

$$B = (a_2\, b)/(a_2 + b)$$

and has a width w at half intensity which is given by

$$w = (1.66)/\sqrt{B}$$

which is related to the widths x and y of the component distributions as

$$w^2 = x^2 + y^2$$

where

$$x = (1.66)/\sqrt{a_2}$$
$$y = (1.66)/\sqrt{b}$$

Therefore, in two crystal spectrometer, in parallel setting one has

$$w' = \sqrt{w_o^2 + w_1^2} \qquad (37)$$

and

$$w = \sqrt{w_1^2 + w_2^2} \qquad (38)$$

where;

w' = overall divergence of the relected beam from the first crystal

w_o = divergence of the reflected beam from the first crystal due to dispersion in this crystal

w_1 = mosaic spread of the first cyrstal

w_2 = mosaic spread of the specimen crystal

w = width of the resultant reflection curve from the specimen crystal at half intensity.

In the present experiment, the divergence of the beam from silicon crystal was measured by a photographic method. From the comparison of the widths of the beam on photographs which were taken at distances of 10 cm. and 298 cm

from the silicon cyrstal, the divergence w′ was found as

$$w' = (23 \pm 4)"$$

During the experiment, the (111) reflection from the silicon crystal was used which has a divergence w_o of (21.34)" due to dispersion. Then, from eq (37), value for the mosaic spread w_1 of silicon crystal was found as

$$w_1 = (9 \pm 6)"$$

For the D(+) tartaric acid crystal used, the diffraction profiles were obtained for (002), (-102), (003), (-203), (-303) and (004) reflections. These are shown in Figs (21) and the information obtained from these graphs is shown in Table (9). The width of the diffraction profiles and $K(\alpha_1 - \alpha_2)$ seperation were increasing with increasing θ as was expected, since dispersion increases with increasing θ. The values found for (002) and (-102) reflections are free from dispersion, since these reflections correspond to nearly parallel setting of two crystal spectrometer. In these cases, the width of the diffraction profiles w, was found to be same for both (002) and (-102) reflections and $K(\alpha_1 - \alpha_2)$ seperation was zero, again as was expected. The value of w was found to be:

$$w = (24 \pm 2)"$$

This value can be taken as the upper limit for mosaic spread of D(+) tartaric acid, assuming that silicon crystal is ideally perfect. Assuming silicon crystal has a mosaic spread, using eq. (38) and the value obtained for w_1, the lower limit for the mosaic spread of D(+) tartaric acid was found as

$$w_2 = (22 \pm 6)"$$

As stated before, silicon crystal used has zero

dislocation density as quoted by the manufacturers and it is reasonable to accept it as ideally perfect crystal. The measurment of divergence of the beam from this cyrstal was very difficult because the photographs of the beam did not have sharp outlines due to air scattering. Under these circumstances it is unlikely that the mosaic spread of D(+) tartaric acid would be less than 26" of arc or more than 22" of arc.

We can now compare this result with the value obtained from Zachariasen's equation assuming type I extinction

$$g_{cu} = (2.8 \pm 0.002) \times 10^4$$

giving a half-width, w_{cu}, of

$$w_{cu} = (5 \pm 0.01)"$$

and

$$g_{Mo} = (1.14 \pm 0.12) \times 10^4$$

$$w_{Mo} = (12 \pm 2.5)"$$

The half-width from the different radiations are significantly different which may again reflect the lack of angle dependence in Zachariasen's equations. These values are of less than the experimental widths, by at least a factor of two but, taking into account the possible errors in Zachariasen's equations and the effect of any primary extinction present, it must be conclu ded that the extinction could be of type I.

Conclusions

From a comparison of the agreements between the extinction parameters obtained using the two radiations, it appears that the extinction was mainly of the secondary type, the standard deviations in the parameters being 8% for secondary extinction and 14% for primary extinction, although those deviations must in part be due to the errors

in the assumed kinematic structure factors. The increase in the extinction as the thickness of the crystals increases also strongly suggests that the extinction is, at least partly, path dependent, i.e. secondary extinction.

The block sizes obtained assuming only type II secondary extinction to be present have been shown to be incompatable with the measured dislocation density, showing the crystal can not be of this type. The block sizes obtained assuming primary extinction is close to the experimental value.

The mosaic spreads of the crystal obtained assuming a type I crystal were of the same order of magnitude as the experimental value. It is therefore likely that the extinction is mainly type I secondary extinction but some primary extinction may be present.

REFERENCES

Abrahams,S.C.,Hamilton,W.C.and Mathieson,A.McL. Acta Cryst. A26(1970),1

Bacon,C.E.and Lowde,R.D. Acta Cryst. 1(1948),303

Becker,P.J.and Coppens,P. Acta Cryst. A30(1974),129

Becker,P.J.and Coppens,P. Acta cryst. A30(1974),148

Borrmann,G. Physik.Z. 42(1941),157

Bragg,W.L.,James,R.W.and Bosanquet,C.H. Phil.Mag. 42(1921),1

Bragg,W.L.,James,R.W.and Bosanquet,C.H. Phil.Mag. 41(1921),309

Brown,D.B. and Fatemi,F. J.Appl. Phys. 45(1974),1544

Cooper,M.J. Acta Cryst. A26(1970),208

Cooper,M.J.,Rouse,K.D. Acta Cryst. A26(1970),214

Cooper,M.J.and Rouse,K.D. Acta Cryst. A27(1971),622

Cooper,M.J.,Rouse,K.D.and Willis,B.T.M. Acta Cryst.A24(1968)484

Darwin,C.G. Phil.Mag. 27(1914),315

Darwin,C.G. Phil.Mag. 27(1914),675

Darwin,C.G. Phil.Mag. 43(1922),800

Denne,W.A. Acta Cryst. A28(1972),192

Hamilton,W.C. Acta Cryst. 10(1957),629

Hamilton,W.C. Acta Cryst. 16(1963),609

Haruta,K. J.Appl.Phys. 36(1965),1789

James,R.W. The Optical Principles of the Diffraction of X-rays (1950)
London:Bell

Killean,R.C.G.,Lawrence,J.L.and Sharma,V.C. Acta Cryst. A28(1972),405

Lang,A.R. Acta Cryst. 10(1957),252

Lang,A.R. Acta Cryst. 12(1959),249

Larson,A.C. Crystallographic Computing (1969).Edited by F.R.Ahmed
Copenhagen:Munksgaard

Lawrence,J.L. Acta Cryst. A28(1972),400

Lawrence,J.L.Acta Cryst. A29(1973),208

Lawrence,J.L. Acta Cryst. A30(1974),454

Mackenzie,J.K. Acta Cryst. A30(1974),607

Maier-Leibnitz,H. Proceedings of the Advanced Institude on the Experimental Aspects of X-ray and Neutron Diffraction (1972). Aarhus-Denmark

Okaya,Y.and Stemple,N.R. Acta Cryst. 21(1966),237

Werner,S.A. Acta Cryst. A25(1969),639

Werner,S.A. J.Appl.Phys. 45(1974),3246

Zachariasen,W.H. Theory of X-ray Diffraction in Crystals (1945). Newyork: Wiley

Zachariasen,W.H. Acta Cryst. 23(1967),558

Zachariasen,W.H. Acta Cryst. A24(1968a),212

Zachariasen,W.H. Acta Cryst. A24(1968b),324

Zachariasen,W.H. Acta Cryst, A24(1968c),425